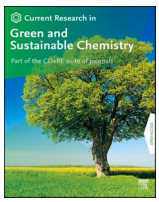
Current Research in Green and Sustainable Chemistry 13 (2026) 100540

Contents lists available at ScienceDirect

Current Research in Green and Sustainable Chemistry

journal homepage: www.elsevier.com/journals/current-research-in-green-and-sustainable-chemistry/2666-0865



Toward zero-waste valorisation of pistachio shells via hydrothermal carbonisation and pyrolysis

Barış Yıldız [a,b], Koray Alper [c], Mustafa Zafer Özel [d,*], İlknur Durukan [a]

[a] Environmental Engineering Department, Hacettepe University, Ankara 06800, Türkiye
[b] Graduate School of Science and Engineering, Hacettepe University, Ankara 06800, Türkiye
[c] Department of Chemical and Chemical Processing Technologies, Çaycuma Food and Agriculture Vocational School, Zonguldak Bülent Ecevit University, Zonguldak 67600, Türkiye
[d] School of Health, Medicine and Life Sciences, University of Hertfordshire, Hatfield AL10 9AB, UK

ARTICLE INFO

Keywords:
Pistachio shell
Zero-waste valorisation
Hydrothermal carbonisation
Pyrolysis

ABSTRACT

The rapid depletion of finite fossil fuels and the traditional linear economic model of "take, make, and dispose" have led to severe environmental degradation and the massive accumulation of underutilised agricultural residues, such as pistachio shells. Concurrently, modern industries face critical ecotoxicological challenges, particularly from the widespread use of synthetic dyes in aquatic environments. Recovering valuable products from waste, commonly known as valorisation or upcycling, is a fundamental aspect of the circular economy, enabling the conversion of discarded materials into high-value resources. To effectively address these intertwined ecological issues, this research implements a zero-waste valorisation strategy for pistachio shells via hydrothermal carbonisation (250–300 °C) and dry pyrolysis (400–500 °C). Rather than relying on conventional single-product recovery, a multi-product approach was utilised. A key innovation involves conditioning the complex liquid phase with a macroporous adsorbent resin, overcoming inherent analytical limitations to successfully recover a stabilised, phenolic-rich biochemical stream. Simultaneously, the solid biochar synthesised at 500 °C demonstrated exceptional dual-purpose utility. It exhibited a high-grade heating value of 31.81 MJ/kg and acted as a robust environmental adsorbent, achieving >96% removal of methylene blue without requiring harsh chemical activation. Equilibrium data conformed to the Freundlich model ($R^2 > 0.999$), indicating heterogeneous multilayer adsorption governed synergistically by π- π interactions, electrostatic forces, and enhanced macroporosity. Ultimately, this employing distinct thermochemical routes proves that dense agricultural waste can be completely transformed into valuable biochemicals, sustainable energy, and advanced carbon materials without generating secondary hazardous effluents.

1. Introduction

The rapid acceleration of global population growth, urbanisation, and industrialisation has triggered an unprecedented demand for energy and chemical resources [1,2]. For decades, economic development has heavily relied on finite fossil fuels, while traditional waste management has followed a linear economic model characterised by "take, make, and dispose". This unsustainable paradigm has resulted in severe environmental consequences, including greenhouse gas emissions, soil degradation, and the massive accumulation of agricultural and industrial residues [3]. To effectively address these interconnected ecological and industrial bottlenecks, a global paradigm shift towards a circular bioeconomy is imperative. Within this framework, the zero-waste concept redefines agricultural residues not as environmental burdens, but as abundant, renewable precursors that must be fully integrated back into the production cycle, emphasising advanced recovery and recycling over low efficiency incineration or landfilling [4,5].

Among various agricultural sectors, the pistachio industry generates a substantial volume of localised lignocellulosic waste. Globally, countries such as the United States, Iran, and Türkiye dominate pistachio production, with Türkiye's yield heavily concentrated in the Southeastern Anatolia Region [5,6]. The processing of pistachios generates hundreds of thousands of tons of hard shell waste annually, which constitutes up to 45% of the total nut weight [7]. Currently, these shells are predominantly considered low-value byproducts and are discarded or burned inefficiently [3,8]. However, pistachio hard shells are dense

* Corresponding author.
E-mail address: m.ozel@herts.ac.uk (M.Z. Özel).

https://doi.org/10.1016/j.crgsc.2026.100540
Received 19 June 2026; Received in revised form 15 October 2026; Accepted 22 October 2026
Available online 28 October 2026
2666-0865/© 2026 Published by Elsevier B.V. This is an open access article under the CC BY-NC-ND license (http://creativecommons.org/licenses/by-nc-nd/4.0/).

lignocellulosic materials characterised by an exceptionally low ash content and a naturally higher heating value (HHV) of 16.85–17.47 MJ/kg [9,10]. Furthermore, their structural matrix is uniquely rich, fundamentally composed of cellulose (38–54%), hemicellulose (15–32%), and a notably high lignin content ranging from 20% to 30% [6,11]. This specific, carbon-rich and highly lignified chemical composition makes pistachio shells highly promising feedstocks for advanced thermochemical biorefineries.

Thermochemical conversion technologies, primarily pyrolysis and hydrothermal processes, offer rapid and highly efficient pathways for transforming dense lignocellulosic biomass into value-added energy and chemical products [12]. Pyrolysis thermally decomposes biomass in an oxygen-free environment, yielding biochar, bio-oil, and syngas [1]. Conversely, hydrothermal carbonisation (HTC) utilises pressurised subcritical water at moderate temperatures, allowing for the conversion of wet biomass without the need for energy-intensive pre-drying [13]. Both processes degrade the macromolecular network of the biomass, yet their distinct operational environments lead to different product distributions [14]. However, traditional applications of these thermochemical technologies often focus on single product recovery, leaving secondary waste streams underutilised, which inherently contradicts the holistic zero-waste philosophy [4].

A significant challenge in realising a multi-product biorefinery lies in the complex chemistry of the generated liquid products [15]. Bio oils and hydrothermal aqueous phases are highly complex, acidic, and heterogeneous mixtures containing hundreds of chemical species, including organic acids, ketones, aldehydes, and heavy pyrolytic oligomers [16]. While the intensive thermal depolymerisation of the high lignin fraction generates exceptionally valuable monomeric phenolic compounds, the presence of heavy tars and highly polar impurities causes severe chemical instability and poses major obstacles for direct analytical characterisation [16]. Therefore, downstream conditioning is mandatory. Utilising macroporous adsorbent resin columns has emerged as an innovative and highly effective pretreatment strategy [17]. By selectively adsorbing hydrophobic aromatic molecules and filtering out highly polar aqueous impurities, resin treatments successfully stabilise and refine the complex liquid matrix, enabling high-resolution identification of targeted platform biochemicals via chromatographic techniques [17,18]. Simultaneously, the carbonaceous solid residues pyrolytic biochar and hydrochar present immense potential for both energetic and environmental applications [19,20]. During carbonisation, intensive deoxygenation and devolatilization mechanisms actively expel oxygen and hydrogen from the solid matrix, dramatically densifying the carbon content and upgrading the raw precursor into an energy-dense solid fuel [19]. Beyond their energetic utility, the rigorous thermal cracking, especially during high temperature pyrolysis, creates a highly interconnected porous network [8]. Combined with the retention of specific oxygen-containing functional groups, this structural evolution transforms the biochar into a robust, reactive adsorbent capable of removing severe ecotoxicological pollutants, such as synthetic methylene blue dye, from aqueous industrial environments [8,19].

In this study, the fundamental purpose is to achieve the holistic zero-waste valorisation of pistachio hard shells by integrating distinct hydrothermal (250–300 °C) and pyrolytic (400–500 °C) conversion pathways. Rather than focusing on a single product, a true multi-product biorefinery concept was implemented to ensure every output phase is optimised. A primary objective within this framework is the selective recovery and purification of high-value phenolic compounds from the complex thermochemical liquid streams. To achieve this, a specially conditioned macroporous adsorbent resin was implemented to refine the liquid phases, systematically reducing non-phenolic impurities to ensure the high purity isolation and accurate classification of these target biochemicals via GC-MS and HPLC analysis. Concurrently, the study systematically evaluates the resulting solid carbonaceous residues as dual-purpose materials. The biochar and hydrochar is comprehensively assessed both for its energetic potential as a high calorific alternative solid fuel and for its environmental utility as a highly effective, non chemically activated adsorbent for the removal of toxic methylene blue dye from aqueous solutions.

2. Materials and methods

2.1. Raw material preparation

The pistachio shells utilised in this study were procured from local agricultural producers in the city of Gaziantep, Türkiye. To isolate the targeted lignocellulosic fraction, the soft outer hulls (mesocarp) and inner kernels were systematically removed, yielding the pure hard shells (endocarp). The isolated shells were pre-dried in a laboratory oven at 60 °C for 24 h to ensure a uniform moisture content and facilitate mechanical processing. Subsequently, the dried biomass was ground using a Retsch SM 200 cutting mill (Haan, Germany) and sieved to obtain a highly homogenous particle size fraction of 1–2 mm. The prepared samples were strictly stored in airtight containers at room temperature to prevent moisture reabsorption before thermochemical processing. The systematic flow of the raw material preparation is illustrated in Fig. 1.

2.2. Biomass conversion

The prepared pistachio shells (1–2 mm) were subjected to two distinct thermochemical conversion pathways: hydrothermal carbonisation (HTC) and dry pyrolysis.

Hydrothermal Carbonisation (HTC): The HTC experiments were performed in a 500 mL high-pressure batch reactor Parr 4848 (Moline, IL, USA). For each experimental run, 15 g of the raw biomass was dispersed in 150 mL of deionised water. The reactor was sealed and heated to target temperatures of 250 °C and 300 °C under autogenous pressure. Following the reaction and subsequent cooling, the solid hydrochar was separated from the highly complex aqueous post-conversion liquid phase via filtration and thoroughly washed sequentially with deionised water, acetone, and ethanol to remove any residual soluble organic compounds and surface-adhered liquid phase residues prior to subsequent characterisation and adsorption tests.

Pyrolysis: The dry pyrolysis process was conducted using a custom-designed stainless steel fixed-bed reactor (6 cm in diameter and 21 cm in height). To maintain a strictly oxygen-free environment and continuously sweep the evolved pyrolytic vapours, a steady flow of nitrogen gas was introduced into the system. The reactor was operated at target temperatures of 400 °C and 500 °C. The volatile products were directed through a multi-stage condensation system cooled with an ice water mixture to maximise the recovery of the liquid fraction (bio-oil), while the solid biochar residue was recovered from the reactor bed. The schematic configuration of the pyrolysis experimental setup is presented in Fig. 2.

2.3. Adsorptive treatment of the post-conversion liquid phase

The liquid products derived from both hydrothermal carbonisation and pyrolysis are complex multicomponent mixtures that pose significant challenges for direct chromatographic analysis due to the presence of heavy oligomeric fractions and highly polar impurities. To refine and stabilise these liquids before characterisation, an adsorptive treatment utilising a macroporous resin column was implemented as a crucial conditioning step.

2.3.1. Preparation of the resin packed column system

A glass chromatography column (15 × 200 mm) was packed with 15 g of SEPLITE LXA88 (Sunresin New Materials Co. Ltd., Xi'an, China), a macroporous adsorbent resin specifically engineered for the selective extraction of polyphenols and organic compounds. The resin was



Fig. 1. Systematic flow of the raw material preparation.

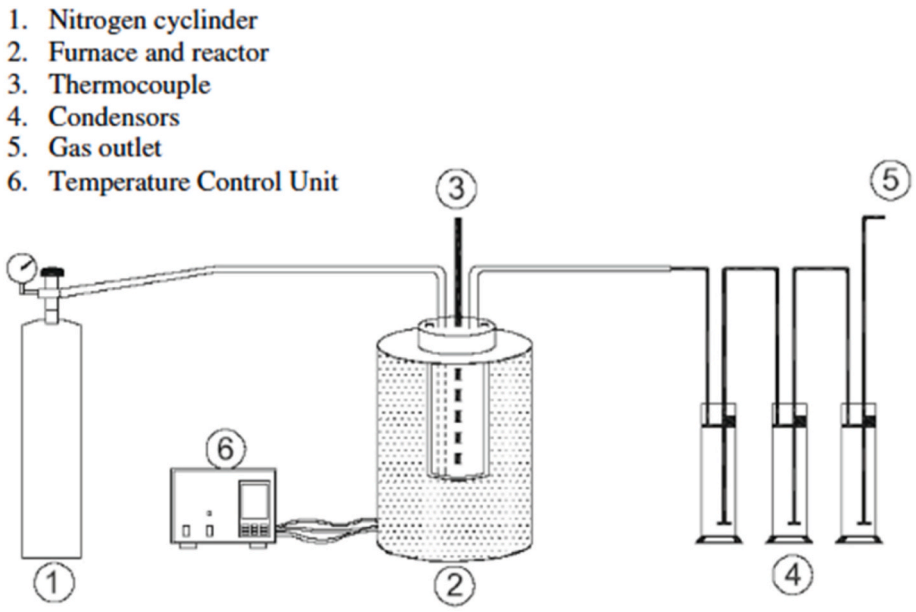


Fig. 2. Pyrolysis experimental setup.

initially mixed with 50 mL of 4% NaOH and loaded into the column, resulting in a stable bed height of 14 cm and a total bed volume (BV) of 25 cm^3. The pretreatment protocol involved passing 3 BV of 4% NaOH at a constant flow rate of 1 BV/h, followed by rinsing with deionised water until the effluent pH dropped below 10. Subsequently, 3 BV of 4% HCl (Merck, Darmstadt, Germany) was introduced into the resin bed at a

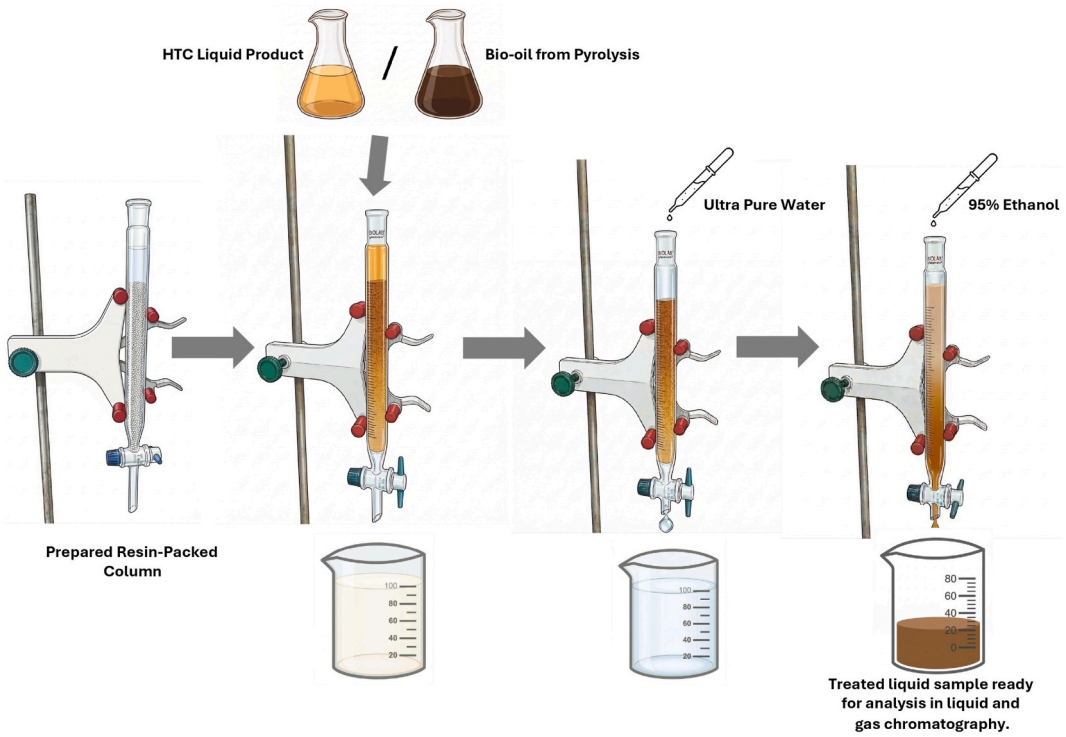


Fig. 3. Elution procedure.

flow rate of 1 BV/h, followed by washing the system with deionised water until the effluent pH rose above 5. For final activation, 3 BV of 95% ethanol was passed through the column to eliminate air bubbles; the resin was soaked in ethanol for 3 h, and then thoroughly washed with deionised water at 1 BV/h, ensuring the resin bed remained submerged at all times.

2.3.2. Column loading and elution procedure

Before column loading, both the hydrothermal post-conversion liquid and the pyrolytic bio-oil were filtered through a 0.45 μm membrane to prevent the potential blockage of resin pores by suspended micro-particles. The filtered liquid samples were systematically loaded onto the activated resin bed at a constant flow rate of 2 BV/h. After completion of the loading process, to effectively eliminate nonadsorbed hydrophilic impurities, such as light organic acids and unretained sugars, the column was thoroughly washed with deionised water at a flow rate of 2 BV/h for 2 h. Finally, the target aromatic and phenolic compounds retained on the hydrophobic sites of the resin were eluted using ethanol. This recovery process was meticulously monitored by tracking the movement of the characteristic coloured band down the column, yielding a standardised volume of 20 mL of the refined eluate for each sample to ensure analytical comparability during subsequent chromatographic measurements. The complete schematic stages of the column loading, the visual monitoring of the coloured fraction, and the elution procedure are illustrated in Fig. 3.

2.4. Characterisation of the treated liquid phase

Following the adsorptive refinement and stabilisation of the liquid products, the chemical composition of the resulting ethanol eluates was systematically analysed to establish a comprehensive chemical fingerprint of the refined fraction. A complementary analytical strategy was implemented utilising both Gas Chromatography-Mass Spectrometry (GC-MS) and High-Performance Liquid Chromatography (HPLC). GC-MS was primarily utilised for the qualitative and semi-quantitative identification of volatile and semi-volatile organic compounds, specifically targeting the phenolic-rich aromatic fractions, while HPLC provided essential data on the distribution of polar and non-volatile oxygenated compounds.

2.4.1. GC-MS analysis

The qualitative and semi-quantitative chemical identification of the volatile and semi-volatile organic compounds was performed using an Agilent 6890 N GC system coupled with an Agilent 5973 N Mass Selective Detector (MSD). Chromatographic separation was achieved using a high-resolution HP-5MS capillary column (60 m × 0.25 mm × 0.25 μm). Helium was utilised as the carrier gas, and the injector was operated in split mode with a split ratio of 1:20 at a constant inlet temperature of 290 °C. The GC oven temperature was precisely programmed with an initial temperature of 50 °C (held for 5 min), followed by a ramp of 3.00 °C/min to 180 °C (held for 4 min), a second ramp of 2.00 °C/min to 200 °C (no hold), and a final ramp of 4.00 °C/min reaching a maximum temperature of 320 °C (held for 5 min), resulting in a total runtime of approximately 97.33 min. The mass spectrometer was operated in electron impact (EI) ionisation mode at 70 eV, and the data were analysed using the National Institute of Standards and Technology (NIST) library for compound identification based on the total ion chromatogram (TIC).

2.4.2. HPLC analysis

HPLC analysis was performed using a Shimadzu Prominence-I LC-2030C Plus HPLC system equipped with an SPD-10A UV-Vis Diode Array Detector (DAD) set at a wavelength of 280 nm to specifically monitor aromatic and phenolic species. The chromatographic separation was conducted on a C18 column (250 × 4.6 mm, 5 μm). An optimised gradient elution method was applied using two mobile phases: 0.1% formic acid in water (Mobile Phase A) and methanol (Mobile Phase B). The analysis was run for 45 min at a constant flow rate of 0.8 mL/min, with a column oven temperature of 30 °C and a total sample injection volume of 20 μL. The gradient elution program was programmed as follows: 30% B from 0 to 15 min; increased to 80% B from 15 to 35 min; and returned to 30% B from 35 to 45 min.

2.5. Characterisation of the solid products and raw biomass

The physical, chemical, and morphological characteristics of the raw pistachio shells and the produced carbonaceous materials (hydrochar and biochar) were comprehensively analysed to evaluate their potential as solid fuels and environmental adsorbents.

2.5.1. Physicochemical and energetic characterisation

Proximate analysis, including moisture, ash, and volatile matter percentages, was determined gravimetrically according to standard protocols (ASTM-D-2016-74, ASTM-D-1102-84, and ASTM-E-872-82, respectively). The ultimate elemental composition (C, H, N, and S) was quantified using a LECO CHNS-932 elemental analyser, with the oxygen content calculated by difference. To evaluate the solid fuel quality, the energy content, represented by the Higher Heating Value (HHV), was experimentally measured using a LECO AC-350 bomb calorimeter.

2.5.2. Structural and morphological characterisation

The surface morphology and structural transformations of the samples were observed using a field emission scanning electron microscope (FE-SEM, FEI Quanta FEG 450). The specific surface area and pore structural characteristics were determined via N_2 adsorption at −196 °C utilising a Micromeritics Gemini VII 2390t analyser. Prior to the BET analysis, the samples were subjected to an intensive "pore-opening" pretreatment using acetone and ethanol, followed by vacuum degassing, to effectively remove any residual pyrolytic tars trapped within the carbon matrix. The crystallographic phase transitions were evaluated by X-ray Diffraction (XRD) using a Rigaku D/MAX 2200 PC diffractometer over a 2θ scanning range of 5° to 80°. Furthermore, the evolution of the surface functional groups was recorded using a Shimadzu IR Spirit Fourier-Transform Infrared (FTIR) spectrophotometer equipped with an ATR accessory, operating between 600 and 4000 cm^{-1} at a spectral resolution of 4 cm^{-1}.

2.5.3. Thermal stability analysis

Thermogravimetric analysis (TGA) was conducted to assess the thermal degradation behaviour and recalcitrance of the solid products. Approximately 7.5 mg of each sample was analysed using a Seiko EXSTAR 7200 TG/DTA instrument. The analysis was performed by heating the samples from ambient temperature to 850 °C at a constant heating rate of 20 °C/min under a continuous nitrogen flow to prevent oxidative degradation.

2.6. Adsorption studies

Batch adsorption experiments were conducted to evaluate the performance of the synthesised biochars and hydrochars for the removal of Methylene Blue (MB), a model cationic dye, from aqueous solutions. For each experimental run, 0.01 g of the biochar/hydrochar was introduced into 50 mL of MB aqueous solution. The mixtures were continuously stirred to ensure adsorption equilibrium. To systematically investigate the adsorption behaviour and the effect of operational parameters, the batch tests were performed under varying contact times, initial dye concentrations, and ambient temperatures. Following the adsorption process, the solid adsorbent was separated from the liquid phase via centrifugation at 4000 rpm for 5 min and subsequent filtration using glass wool. The residual MB concentration in the aqueous phase was quantified using a Thermo Scientific Genesys 10S UV-Vis

spectrophotometer at a maximum absorption wavelength (λ_{max}) of 665 nm. The equilibrium adsorption capacity (q_e, mg/g) and the dye removal efficiency (R%) were calculated using the following mass balance equations [21]:

$$q_e = \frac{(C_0 - C_e)\, x\, V}{m} \quad (1)$$

$$R\% = \frac{(C_0 - C_e)}{C_0}\, x\, 100 \quad (2)$$

where C_0 and C_e represent the initial and equilibrium MB concentrations (mg/L), respectively, V is the volume of the dye solution (L), and m is the mass of the biochar/hydrochar used (g). Furthermore, to describe the distribution of the dye molecules between the solid and liquid phases, the experimental equilibrium data were systematically fitted to the Langmuir and Freundlich isotherm models.

3. Results

3.1. Temperature-dependent thermochemical transformation of the biomass

Pistachio hard shells were thermochemically converted via hydrothermal carbonisation (HTC) at 250 °C and 300 °C, and dry pyrolysis at 400 °C and 500 °C to observe the macroscopic product distributions. For the HTC process (using 15 g biomass in 150 mL water), a solid hydrochar was formed alongside a large volume of recovered liquid phase (145–150 mL). As the temperature increased from 250 °C to 300 °C, the hydrochar yield naturally decreased due to enhanced thermal degradation and the solubilization of organic intermediates. Conversely, dry pyrolysis yielded a solid biochar and a highly condensed liquid fraction (bio-oil) of approximately 8–10 mL. Overall, the distinct operational conditions of HTC (wet, moderate temperature) and dry pyrolysis (dry, high temperature) led to significant differences in physical yields, the chemical profiles of which are comprehensively investigated in the subsequent sections.

3.2. Chemical profile of the liquid phase

The liquid products derived from the thermochemical conversion of lignocellulosic biomass represent a highly complex and heterogeneous matrix of oxygenated and non-oxygenated organic species. To overcome the inherent analytical limitations associated with raw bio-oils, such as the presence of heavy pyrolytic oligomers and thermal instability, a macroporous adsorbent resin column pretreatment was systematically applied to all liquid phases. This crucial conditioning step selectively isolated the valuable monomeric fractions and stabilised the matrix by mitigating impurities, thereby ensuring high-resolution chemical profiling.

3.2.1. Semi-quantitative analysis of the liquid phase by GC–MS

The refined liquid extracts from both hydrothermal carbonisation (HTC) and dry pyrolysis were analysed via Gas Chromatography-Mass Spectrometry (GC-MS) to identify and semi-quantify the volatile and semi-volatile organic compounds generated during the thermal breakdown of the pistachio shell biomass. To analyse each GC-MS dataset, these correlating retention times and mass spectra. Each compound in a mixture has a specific retention time that matches the mass spectra when compared with other samples. The percentage of each component is given as the percentage of peak area of the analyte. To systematically interpret the extensive dataset, the identified chemical species were classified into major functional families: phenols, aldehydes, ketones, acids, alcohols, esters, aliphatic/aromatic hydrocarbons, and a broader 'others' category (predominantly nitrogenous and furanic derivatives). The specific chemical compositions and the relative distribution (area %) of these functional groups for each applied temperature are detailed in Tables A1 through A4 in Appendix A.

The structural decomposition of the pistachio shell's dense lignocellulosic matrix profoundly dictated this functional group distribution. Regardless of the applied processing conditions, phenolic compounds emerged as the overwhelmingly dominant chemical family in the refined liquid extracts. This high phenolic yield is a direct chemical consequence of the intensive depolymerisation of the abundant lignin macromolecule. Among these, Phenol, 2,6-dimethoxy- was consistently identified as the primary marker compound across different samples, highlighting the strong phenolic-rich nature of the precursor lignin. In contrast, the carbohydrate polymers primarily decomposed into oxygenated aliphatic fractions, where organic acids originated from the early-stage degradation of hemicellulose, while aldehydes and ketones resulted from the fragmentation of crystalline cellulose. Furthermore, the degradation of structural proteins and secondary cross-polymerisation reactions contributed to nitrogen-containing heterocyclic species and, under extreme deoxygenation, pure hydrocarbons. The applied thermal severity acted as the primary operational driver governing the evolutionary pathways of these chemical species. The temperature-dependent evolution of the functional groups is visually illustrated in the comparative distribution graphs.

Within the subcritical aqueous environment of HTC, the liquid phase exhibited extreme chemical selectivity at 250 °C (Fig. 4), dominated almost entirely by a phenolic fraction (65.11%) and an aldehyde fraction (34.89%). However, elevating the HTC temperature to 300 °C (Fig. 5) triggered a profound chemical shift, causing the complete disappearance of the aldehyde fraction, which was replaced by the emergence of organic acids and a significant nitrogenous fraction. This transition demonstrates that increasing the HTC temperature accelerates secondary aqueous-phase reactions and the aqueous oxidation of early-stage aldehydes.

Conversely, the chemical transition within the dry pyrolysis regime from 400 °C to 500 °C (Figs. 6 and 7) initiated a vastly diversified bio-oil profile driven by massive devolatilization and secondary vapour-phase cracking. At 400 °C, a complex equilibrium of ketones, alcohols, and acids was established. When the pyrolysis severity was elevated to 500 °C, the reaction mechanisms shifted heavily towards intense thermal cracking, marked by the exclusive formation of pure non-oxygenated hydrocarbons (alkanes-alkenes-alkins), which were entirely absent at 400 °C. The successful generation of these hydrocarbons explicitly demonstrates that extreme pyrolytic temperatures forcefully drive deep decarboxylation and decarbonization reactions, actively rejecting oxygen from the matrix.

3.2.2. Effect of column treatment on liquid phase composition

Direct chromatographic analysis of crude thermochemical liquids can lead to significant matrix interferences due to highly polar aqueous compounds and heavy oligomeric tars. Therefore, High-Performance Liquid Chromatography (HPLC) analysis was conducted at 280 nm to comparatively profile the chromatographic fingerprints of the liquid fractions before (aqueous flow-through, H_2O) and after (ethanol eluate, EtOH) the column treatment, specifically targeting aromatic and phenolic species.

The comparison of the chromatograms clearly demonstrates the profound purification and selective adsorption capabilities of the resin column. In the EtOH fractions derived from the resin column treatment, the detected peaks were heavily concentrated, as expected at the very early retention times, indicating the presence of highly polar and hydrophilic compounds (e.g., organic acids or polyphenols). As expected, the chromatograms of the aqueous fractions exhibited a remarkably broader, much less concentrated, and more complex distribution of peaks. The emergence of these well-resolved peaks confirms that the valuable semi-polar and polar aromatic/phenolic compounds were successfully retained by the resin in both selected temperatures (250 and 300 °C) products (Fig. 8). Ultimately, this proves that the column

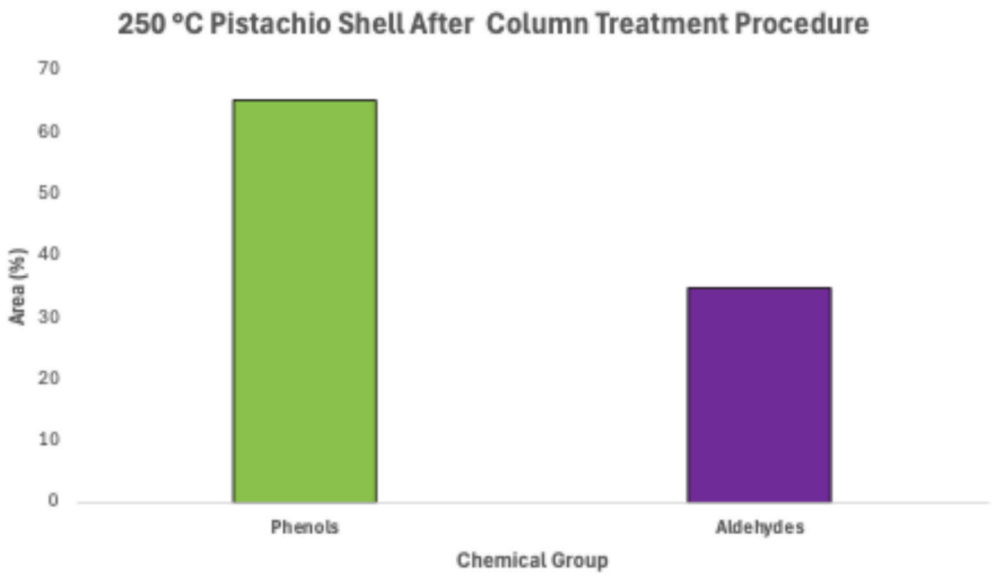


Fig. 4. Functional group distribution of 250 °C HTC liquid product.

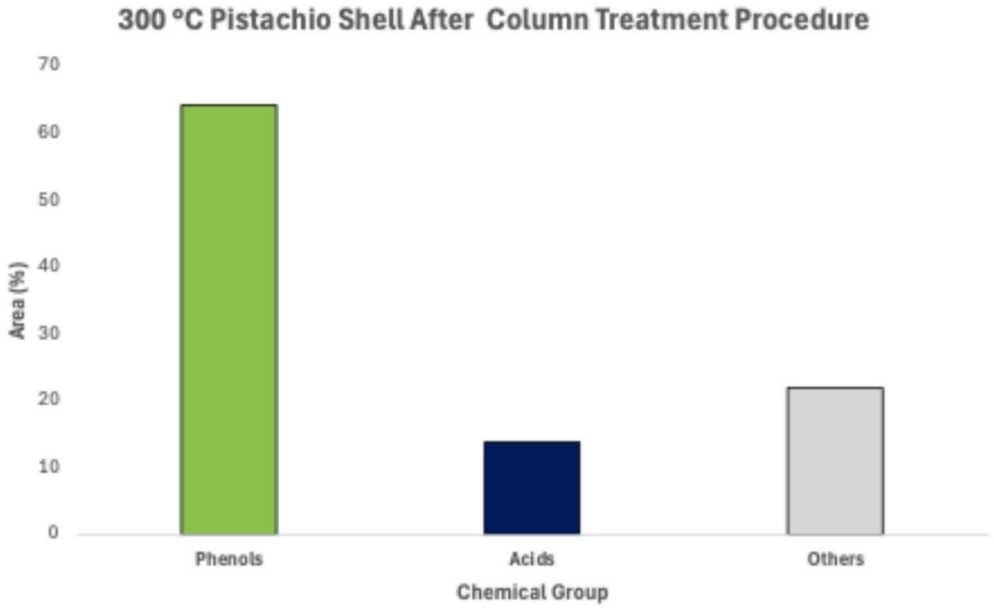


Fig. 5. Functional group distribution of 300 °C HTC liquid product.

treatment acts as a highly effective fractionation mechanism, selectively isolating and concentrating the targeted polar/phenolic compounds while systematically removing some impurities to stabilise the matrix.

3.3. Structural and physicochemical characterisation of solid product

The solid carbonaceous residues generated from the thermochemical conversion of pistachio shells, namely hydrochar from hydrothermal carbonisation (HTC) and biochar from dry pyrolysis, represent highly versatile, value-added materials central to the zero-waste framework of this study. To systematically evaluate their potential as high-energy solid fuels and environmental adsorbents, a comprehensive physicochemical and structural characterisation was conducted.

3.3.1. Proximate and elemental analysis

The fundamental fuel characteristics of the raw pistachio shell precursor were initially assessed via proximate analysis. The raw biomass exhibited a remarkably high volatile matter content of 82.19%, alongside a low moisture content of 5.21% and an exceptionally low ash content of only 1.34%. The massive volatile fraction indicates a rich lignocellulosic matrix primed for extensive devolatilization, while the exceptionally low ash content mitigates the risks of severe slagging and fouling when the resulting biochar/hydrochar is utilised as a solid fuel.

To monitor the extent of carbonisation, the elemental composition (C, H, N, S, and calculated O) of the raw biomass and the resulting solid chars was systematically determined. The raw pistachio shell possessed a relatively low carbon content (45.56%) and a massive oxygen fraction (48.19%). However, thermochemical treatments triggered deep deoxygenation and carbon densification. During HTC, the carbon content surged to 69.55% at 250 °C and 73.10% at 300 °C, primarily driven by intense hydrolysis, dehydration, and decarboxylation reactions that expelled oxygen and hydrogen. The transition to high-severity dry pyrolysis further exacerbated this transformation. At the extreme pyrolytic condition of 500 °C, the carbon content reached its maximum of

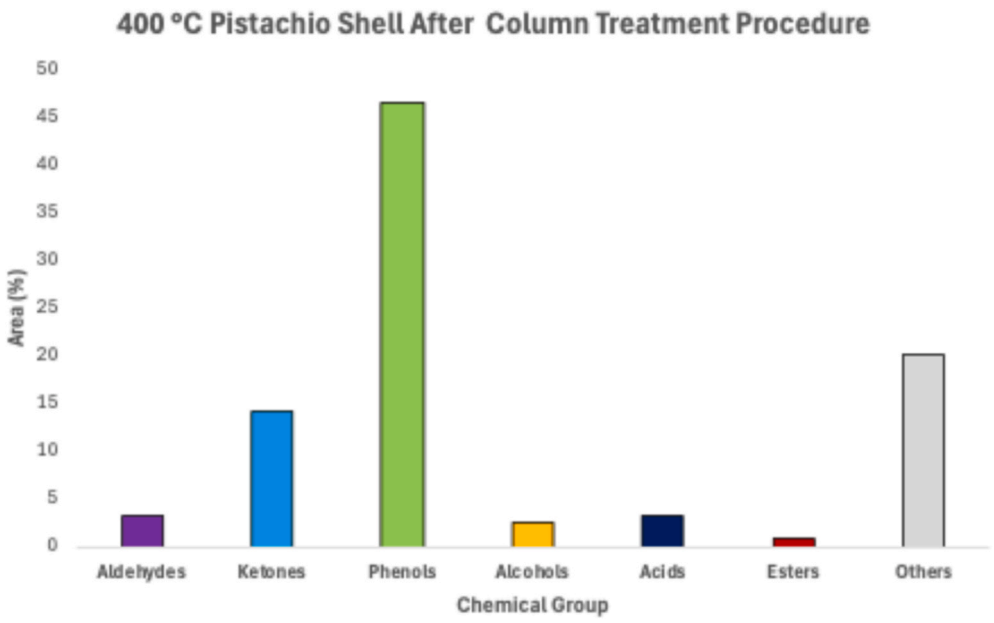


Fig. 6. Functional group distribution of 400 °C pyrolysis liquid product.

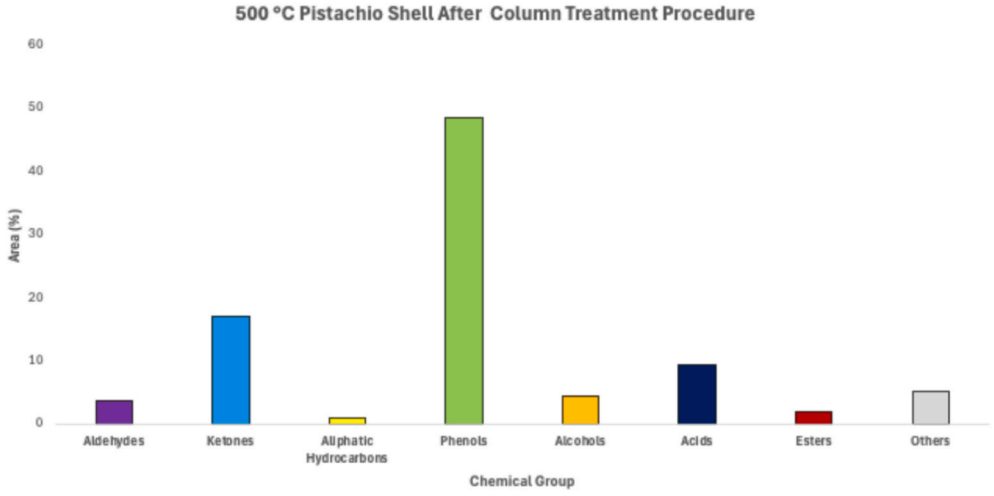


Fig. 7. Functional group distribution of 500 °C pyrolysis liquid product.

82.40%, while the hydrogen and oxygen contents plummeted to 3.36% and 13.74%, respectively. This drastic elemental shift analytically proves the successful upgrading of the agricultural waste into a coal-like solid material.

3.3.2. *Surface and morphological properties (BET and SEM)*

The physical structure, surface area, and porosity of carbonaceous materials are critical parameters that dictate their potential applications. The BET analysis revealed a clear positive correlation between the thermochemical severity and textural development. The hydrochars produced via HTC at 250 °C and 300 °C exhibited moderate BET surface areas of 24.81 m^2/g and 31.56 m^2/g, respectively, associated with the partial hydrolysis and degradation of the biomass. Conversely, high-temperature dry pyrolysis resulted in a more pronounced textural evolution. The biochar produced at 400 °C showed a significantly enhanced surface area of 53.89 m^2/g, which further increased to a peak value of 61.03 m^2/g at 500 °C.

These quantitative surface area results are highly consistent with the morphological transformations observed via SEM, the micrographs of which are provided in Appendix B. While the hydrochars exhibited relatively dense and agglomerated surfaces, the SEM micrograph for the 500 °C biochar clearly demonstrates an interconnected, macroporous honeycomb-like morphology. This structural opening proves that high-temperature pyrolysis successfully upgrades the dense shell into an active biochar matrix.

3.3.3. *Structural evolution (XRD and FTIR)*

The crystallographic transformations and the evolution of surface chemical functional groups were tracked using XRD and FTIR spectroscopy. The XRD diffractogram of the raw biomass exhibited typical distinct diffraction peaks around $2\theta \sim 16°$ and 22°, corresponding to the crystalline planes of native cellulose. Following HTC at 250 °C and 300 °C, the intensity of these cellulose peaks noticeably decreased, confirming successful subcritical hydrolysis. However, the most dramatic structural metamorphosis occurred during high-severity dry pyrolysis. At 400 °C and 500 °C, the characteristic crystalline cellulose peaks completely vanished and were replaced by a broad, diffuse diffraction band in the range of $2\theta \sim 20°–25°$. This proves that extreme

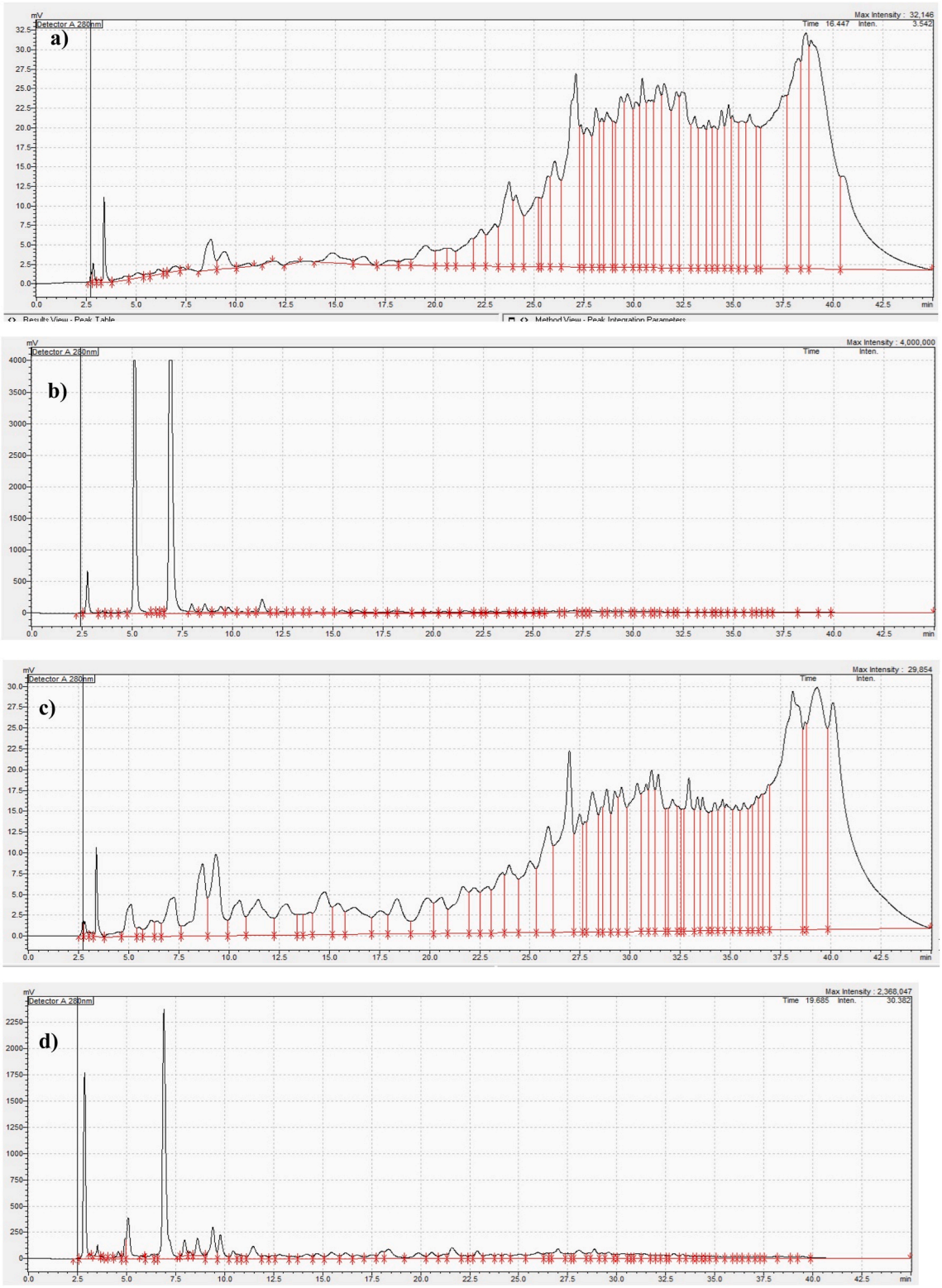


Fig. 8. Comparative HPLC chromatograms (recorded at 280 nm) of the aqueous flow-through (H2O) and ethanol-eluted (EtOH) fractions derived from the resin column treatment of the liquid products obtained at 250 °C and 300 °C. a) HPLC chromatogram of 250 °C liquid product before resin treatment b) HPLC chromatogram of ethanol after resin treatment of the 250 °C liquid product. c) HPLC chromatogram of 300 °C liquid product before resin treatment. d) HPLC chromatogram of ethanol after 300 °C liquid product's resin treatment.

thermal cracking obliterated native crystallinity and repolymerized the carbon into a condensed, disordered aromatic matrix (Fig. 9).

The corresponding FTIR spectra, detailed in Appendix C, mirrored this crystallographic destruction. In the hydrochars (250 °C and 300 °C), polar binding sites significantly survived, providing essential sites for the robust chemisorption of cationic pollutants. In stark contrast, extreme pyrolytic conditions (400 °C and 500 °C) resulted in the near-complete flattening of the spectra, eliminating O–H and aliphatic C–H

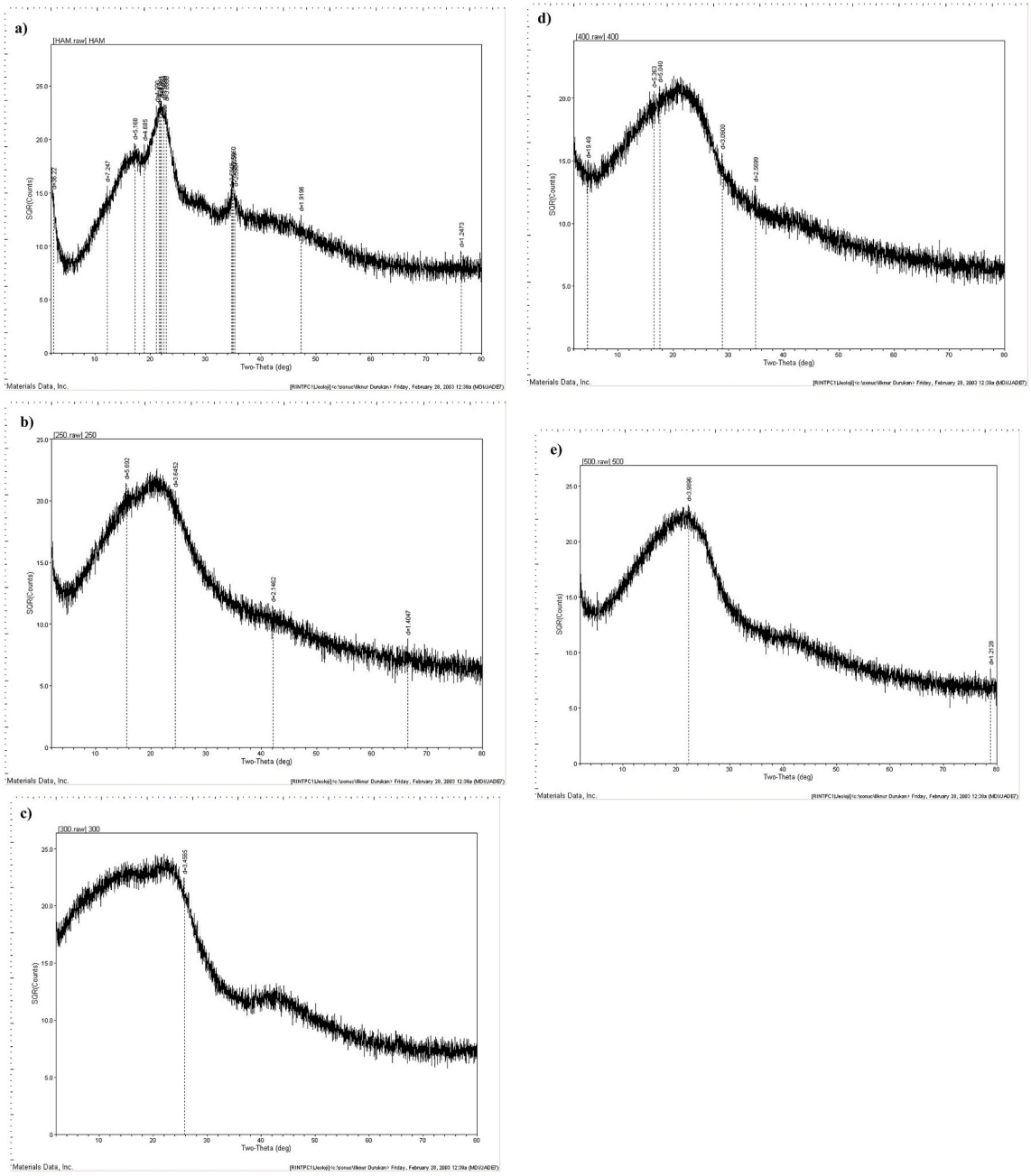


Fig. 9. XRD diffractogram of solid products a) raw pistachio shells, b) 250 °C hydrochar c) 300 °C hydrochar, d) 400 °C biochar, e) 500 °C biochar.

bands while promoting aromatic C═C stretching vibrations (~1600 cm^{-1}). This aromatisation enables the powerful π−π electron interactions responsible for advanced dye adsorption capacity.

3.3.4. *Thermal stability*

Thermogravimetric analysis (TGA) was conducted under an inert nitrogen atmosphere to evaluate the structural recalcitrance of the samples, with the corresponding thermogravimetric (TG) and derivative thermogravimetric (DTG) curves presented in Appendix D.

The raw biomass exhibited a massive and rapid mass loss predominantly between 250 °C and 400 °C, yielding a remarkably low final solid residue of only ~21 wt% at 800 °C. The application of thermochemical treatments systematically enhanced the stability of the carbonaceous matrix. For the hydrochars (250 °C and 300 °C), the initial hemicellulose degradation shoulder was eliminated, and the solid residues at 800 °C increased significantly to ~47 wt% and ~52 wt%, respectively. The transition to high-severity dry pyrolysis resulted in the ultimate degree of thermal recalcitrance. The intense devolatilization and aromatisation mechanisms culminated in exceptionally high final solid residues at 800 °C, recording ~70 wt% for the 400 °C biochar and nearly ~79 wt% for the 500 °C biochar, closely mimicking the thermal behaviour of high-rank coals.

3.3.5. *Energy potential assessment*

To quantitatively evaluate the solid fuel quality of the synthesised materials, the higher heating values (HHV) were experimentally determined. Unprocessed pistachio shells typically exhibit a moderate HHV ranging between 16.85 and 17.47 MJ/kg. The HHV of the raw shell was calculated as 15.16 MJ kg^{-1} based on the elemental analysis results using the empirical equation HHV (MJ kg^{-1}) = (0.338 × C) + 1.428 × (H − O/8) + (0.095 × S), where C, H, O, and S represent the elemental contents of carbon, hydrogen, oxygen, and sulphur, taken from Table 1,

Table 1
Table of elemental analysis results.

Process Conditions	C (wt %)	H (wt %)	N (wt %)	S (wt %)	O[a] (wt %)	H/C[b]	O/C[b]
Raw Shells	45.56	5.85	0.26	0.14	48.19	1.54	0.79
250	69.55	4.87	0.41	0.15	25.02	0.84	0.27
300	73.10	4.91	0.48	0.07	21.44	0.81	0.22
400	75.77	4.13	0.27	0.10	19.73	0.65	0.20
500	82.40	3.36	0.48	0.02	13.74	0.49	0.13

[a] Oxygen content calculated by difference (100 - (C + H + N + S)).
[b] Atomic ratios.

respectively. However, the thermal treatments induced a profound energy densification process across all applied severities.

During HTC, the HHV reached 27.80 MJ/kg at 250 °C and 29.47 MJ/kg at 300 °C. The transition to high-severity dry pyrolysis resulted in even more pronounced upgrading. The biochar produced at 400 °C recorded an impressive HHV of 31.07 MJ/kg, while the absolute maximum energy content of 31.81 MJ/kg was achieved at 500 °C. This peak value makes the 500 °C biochar energetically comparable to high-rank fossil fuels, such as bituminous coal or anthracite. The progressive and drastic increase in the HHV aligns with the elemental densification and thermal stability trends, analytically proving that the zero-waste paradigm successfully upgrades low-value agricultural residues into sustainable, high-calorific alternative solid fuels (Table 2.). The decline in atomic H/C and O/C ratios alongside the substantial increase in HHV up to 31.81 MJ/kg underscores a profound energy densification, confirming that high-severity thermochemical treatments successfully upgrade the raw biomass into high-grade solid fuels comparable to bituminous coal.

3.4. Adsorption performance of biochar and hydrochar

Evaluating the adsorptive performance of the synthesised solid products is a vital pillar of the integrated zero-waste biorefinery concept. While the liquid fraction yields refined platform biochemicals, the solid carbonaceous residue must also be fully valorised to avoid secondary solid disposal, establishing a dual-purpose application framework for energy and environmental remediation. The potential of the synthesised solid carbonaceous materials, ranging from low-temperature hydrochars to high-temperature biochars as robust environmental adsorbents was comprehensively evaluated through the removal of Methylene Blue (MB), a widely utilised model cationic dye, from aqueous solutions. To systematically assess their practical applicability and to elucidate the underlying interactive mechanisms, the influence of fundamental operational parameters and thermodynamic isotherm models was investigated.

3.4.1. Effect of experimental parameters

The operational efficiency of the synthesised chars was systematically evaluated under varying contact times, initial dye concentrations, pH levels, and ambient temperatures.

3.4.1.1. Effect of adsorption time. The effect of contact time on the remaining MB concentration, utilising the chars produced at different thermal severities, is visually illustrated in Fig. 10. The kinetic evaluation revealed a biphasic adsorption behaviour across all tested adsorbents. The removal of the cationic dye proceeded at a remarkably rapid rate during the first 40 to 60 min, primarily driven by the abundance of accessible, vacant active binding sites on the external surface and a strong initial concentration gradient. As the contact time progressed, the rate of adsorption gradually decelerated, indicating a transition from rapid surface attachment to a slower intraparticle diffusion stage. A state of absolute dynamic equilibrium was conclusively attained at 120 min, after which the residual dye concentration formed a highly stable plateau. The biochar produced at the highest pyrolytic severity (500 °C) exhibited the most superior kinetic performance, hierarchically following the order of 500 °C > 400 °C > 300 °C > 250 °C. This exceptional efficiency is directly linked to the violent devolatilization experienced during high-temperature pyrolysis, which generated an interconnected macroporous structure, providing unhindered diffusion pathways for the bulky MB molecules.

3.4.1.2. Effect of initial concentration of adsorbate. The initial concentration of the adsorbate fundamentally alters the mass transfer driving force. As illustrated in Fig. 11, increasing the initial MB concentration from 1 mg/L to 5 mg/L resulted in a slight decline in the overall removal percentage (from 97.00% to 96.43% for the 500 °C biochar) due to the saturation of available surface sites. However, the actual equilibrium adsorption capacity (q_e) surged dramatically from 4.85 mg/g to an impressive 24.11 mg/g, confirming that higher concentrations effectively overcome mass transfer resistances, pushing more dye molecules deep into the biochar's porous network.

3.4.1.3. Effect of pH. From a practical operational standpoint, the synthesised biochars/hydrochars demonstrated remarkable chemical stability across different pH levels, as depicted in Fig. 12. The removal efficiency was found to be relatively insensitive to pH variations, recording 96.15% at pH 4 and stabilising at approximately 96.40% between pH 5 and 10 for the 500 °C biochar. This consistent performance across a broad pH range eliminates the need for costly and time-consuming pH adjustment steps in real wastewater treatment applications.

3.4.1.4. Effect of temperature. Furthermore, the effect of ambient temperature (30, 40, 50, and 60 °C) was investigated to evaluate the thermodynamic nature of the adsorption system, with the results presented in Fig. 13. Varying the temperature yielded only a marginal increase in the removal efficiency (from 96.43% to 97.08% for the 500 °C biochar), suggesting a slightly endothermic process. Energetically, this proves that the biochar/hydrochar performs exceptionally well at standard room temperature (30 °C), requiring no additional thermal energy to achieve maximum efficiency.

3.4.2. Isotherm modelling

Adsorption isotherms provide essential mathematical insights into the interactive behaviour and distribution of the dye molecules between the liquid and solid phases at equilibrium. The experimental equilibrium data were evaluated using the Langmuir and Freundlich macroscopic models. The linear fitting plots for the Freundlich and Langmuir isotherms are presented in Figs. 14 and 15, respectively, with all calculated thermodynamic constants systematically summarised in Table 3.

As explicitly detailed in Table 3 and visually supported by the linear plots in Fig. 14, the Freundlich model provided an exceptionally precise and dominant fit for all synthesised chars, with correlation coefficients (R^2) exceeding 0.999. This near-perfect linearity strongly indicates that the adsorption of MB occurs on a highly heterogeneous surface via multi-layer interactions. Furthermore, the Freundlich intensity parameter (n) was consistently greater than 1, analytically confirming a highly favourable adsorption process. The relative adsorption capacity

Table 2
Table of higher heating values.

Process Conditions	Sample-1 (cal/g)	Sample-2 (cal/g)	Standard Deviation	RSD %	Average (cal/g)	Average (MJ/kg)
250 °C	6682.4	6598.2	59.5	0.90	6640.30	27.80
300 °C	7081.6	6994.3	61.7	0.88	7037.95	29.47
400 °C	7451.5	7391.8	42.2	0.57	7421.65	31.07
500 °C	7589.0	7606.3	12.2	0.16	7597.65	31.81

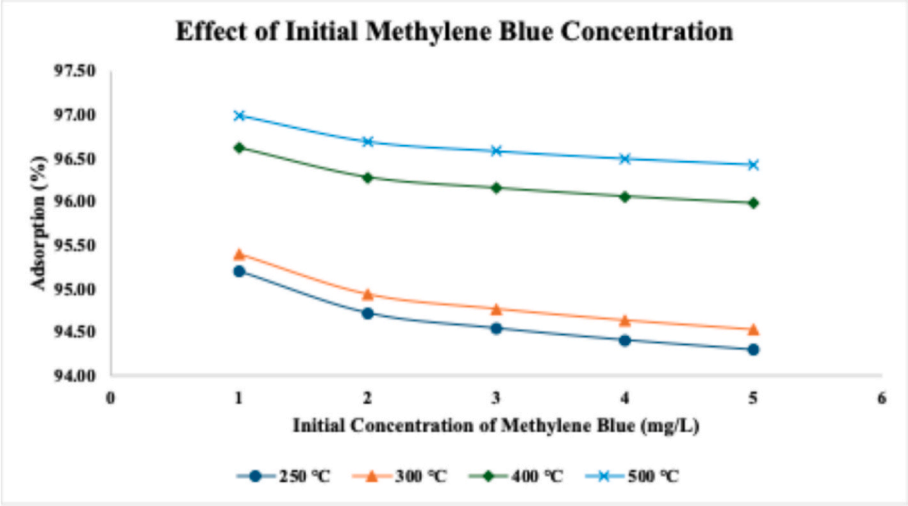


Fig. 10. Effect of initial dye concentration (1–5 mg/L) on the removal efficiency and equilibrium adsorption capacity (q_e) of Methylene Blue for the synthesised carbonaceous materials.

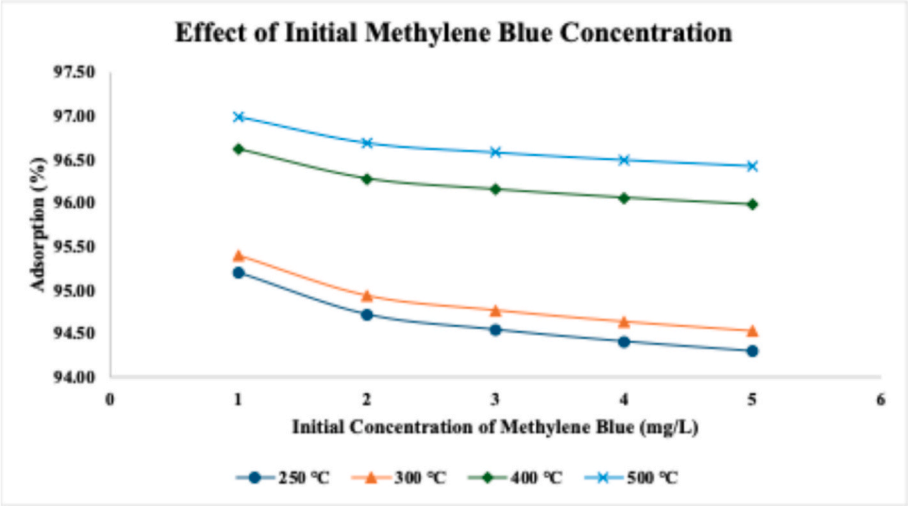


Fig. 11. Effect of initial dye concentration (1–5 mg/L) on the removal efficiency and equilibrium adsorption capacity (q_e) of Methylene Blue for the synthesised carbonaceous materials.

constant (K_f) exhibited a progressive upward trend, surging from 71.72 for the 250 °C hydrochar to a maximum of 111.99 for the 500 °C biochar, quantitatively proving that high-temperature pyrolysis creates a much more capacious active matrix.

In contrast, as depicted in Fig. 15, the linear plots of the Langmuir model exhibited a significantly poorer fit to the experimental data. The much lower R^2 values (0.8807–0.8923) mathematically demonstrate that the homogeneous monolayer assumption of the Langmuir model is inadequate for describing this specific biosorption system. Rather than filling up layer by layer in uniform physical pores, the synthesised hydrochars and biochars function through complex, heterogeneous multi-layer chemical interactions across a highly functionalized carbon network.

3.4.3. Discussion of adsorption mechanism

Based on the combined morphological, chemical, and thermodynamic evidence, the exceptional removal of Methylene Blue by the synthesised carbonaceous materials is not a simple physical pore-filling process, but rather a synergistic combination of multiple interaction mechanisms operating on a highly heterogeneous surface.

The primary driving forces can be identified as follows:

Electrostatic Attraction: The surface of the chars is decorated with oxygen-containing functional groups (proven by FTIR) that deprotonate in the aqueous phase, creating a powerful electrostatic attraction towards the positively charged cationic MB molecules [22].

π−π Electron Interactions: As thermochemical severity increases, the biomass matrix undergoes deep aromatisation (proven by XRD and FTIR), forming a graphite-like carbon network. The delocalized π-electrons on the biochar's aromatic rings strongly interact with the π-electron system of the MB dye structure, creating highly stable surface complexes [23].

Hydrogen Bonding: Residual surface functional groups act as hydrogen donors or acceptors, forming strong hydrogen bonds with the nitrogen and sulphur heteroatoms present in the dye molecules [24].

Physical Pore Filling and Diffusion: As explicitly proven by the SEM micrographs, high-temperature pyrolysis vigorously blows open the dense biomass structure. These newly created interconnected macrotunnels minimise mass transfer resistance, allowing the bulky MB molecules to effortlessly diffuse into the inner matrix and access the internal active binding sites [25].

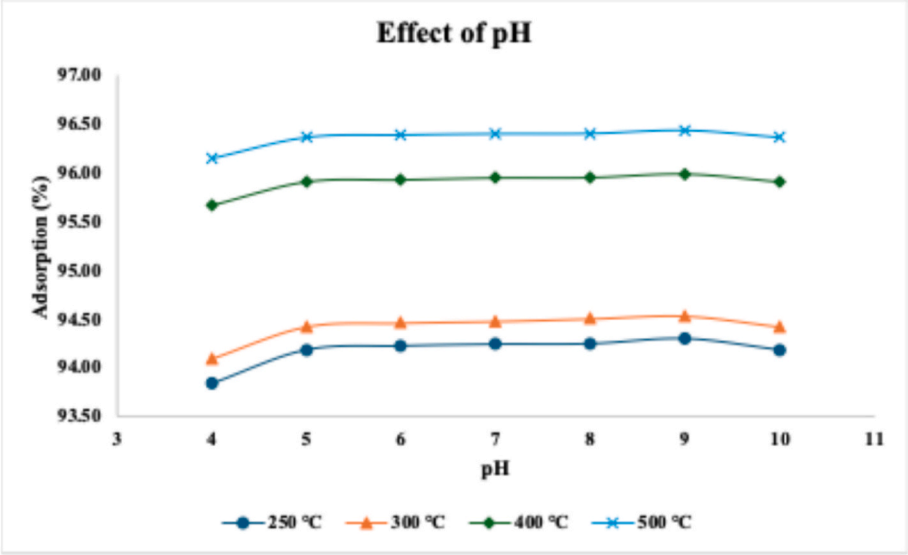


Fig. 12. Effect of initial solution pH (4–10) on the adsorption performance of the synthesised chars.

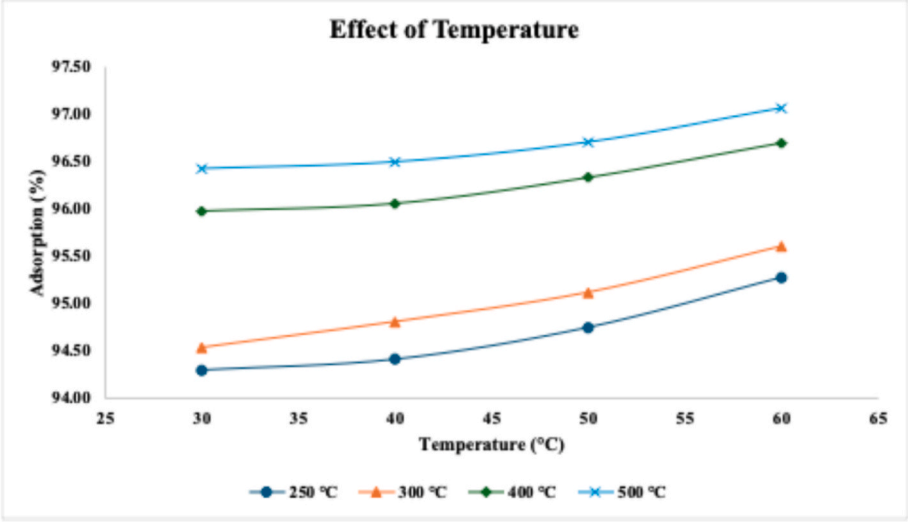


Fig. 13. Effect of ambient temperature (30–60 °C) on the adsorption efficiency of Methylene Blue.

4. Discussion

The exponential increase in global agricultural production and agrifood processing has led to the generation of massive quantities of lignocellulosic residues. Traditionally, the management of agricultural byproducts relied on a linear economic model of "take, make, and dispose," resulting in inefficient incineration or landfilling. However, the modern paradigm of sustainable waste management dictates a transition toward a Circular Bioeconomy, where agricultural residues are viewed as abundant, renewable precursors for advanced biorefineries. The zero-waste valorisation (ZWV) concept builds upon this paradigm, aiming to eliminate final residual waste by ensuring that every fraction of the processed biomass is upgraded into high-value, functional materials. Within the scope of this study, a holistic zero-waste biorefinery approach was successfully designed and executed for the comprehensive valorisation of pistachio hard shells. Instead of employing single-product recovery, this study utilising complementary thermochemical pathways to simultaneously valorise both the solid and liquid phases. The carbonaceous solid fraction was dual-purposed as a high-calorific alternative solid fuel and as a robust environmental adsorbent. Concurrently, the complex liquid fraction (bio-oil) was actively conditioned using an adsorbent resin column to stabilise and refine its phenolic-rich chemical profile, bridging the gap between waste generation and valuable biochemical recovery. To quantitatively and qualitatively assess the novelty and efficiency of the proposed process, it is essential to contextualise the findings against the literature, as summarised in Table 4.

As explicitly demonstrated in Table 4, the vast majority of previous studies predominantly rely on a "single-product" valorisation approach. Numerous studies targeting environmental remediation have utilised nutshells to produce activated carbon using harsh chemical activating agents (such as KOH or $ZnCl_2$). While effective for adsorption, chemical activation inherently contradicts the zero-waste philosophy by generating secondary hazardous and toxic liquid effluents that require extensive washing and neutralisation. Although the maximum BET surface area obtained in this study was 61.03 m^2/g at 500 °C, which is lower than those reported for chemically activated materials derived from other biomass sources in the literature, such as rice straw (275.30 m^2/g), sugarcane bagasse (509.43 m^2/g), and coconut shell (408.59 m^2/g)—this moderate area stems directly from our sustainable,

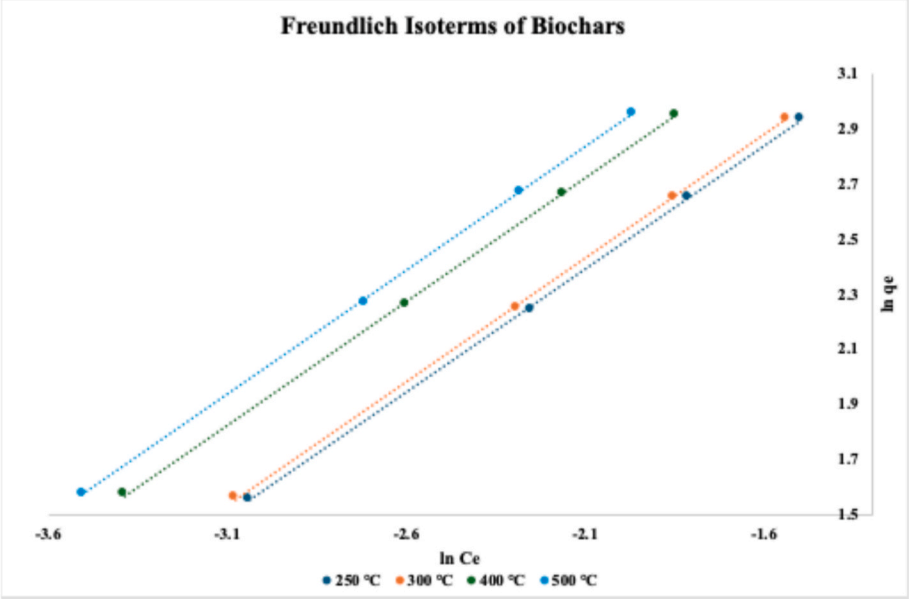


Fig. 14. Linear fitting plots of the Freundlich isotherm model for the adsorption of Methylene Blue onto the synthesised hydrochars and biochars.

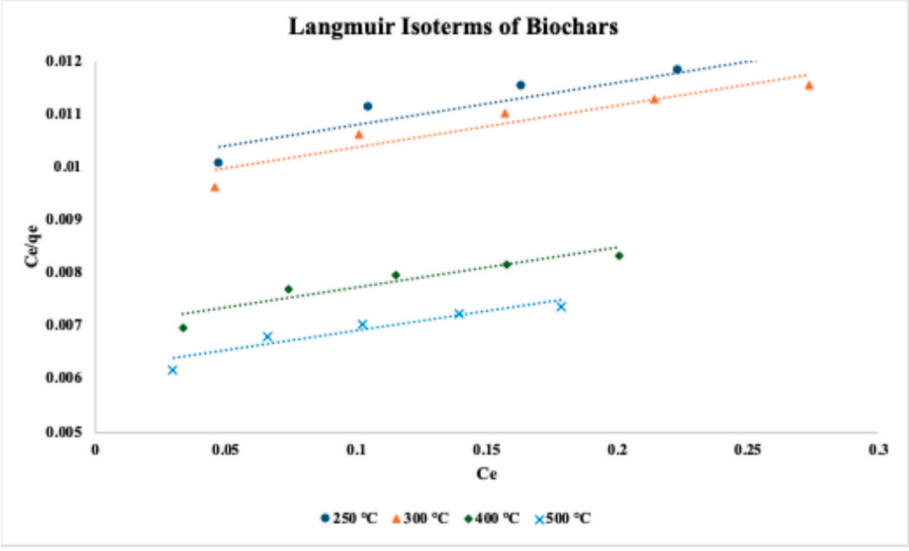


Fig. 15. Linear fitting plots of the Langmuir isotherm model for the adsorption of Methylene Blue onto the synthesised hydrochars and biochars.

Table 3
Langmuir and Freundlich isotherm parameters for the adsorption of Methylene Blue onto the synthesised carbonaceous materials.

Freundlich Isoterm Constants				
	250 °C	300 °C	400 °C	500 °C
K_f [mg/g.(l/mg)$^{1/n}$]	71.72	74.66	100.17	111.99
n	1.117	1.116	1.113	1.115
R^2	0.9998	0.9998	0.9995	0.9997
Langmuir Isoterm Constants				
	250 °C	300 °C	400 °C	500 °C
a (l/mg)	0.7927	0.8244	1.1052	1.2381
b (mg/g)	125.86	126.44	130.04	131.17
r^2	0.8912	0.8923	0.8807	0.8906

chemical-activation-free preparation route [33–35]. In stark contrast, the biochar/hydrochar produced in this study achieved an outstanding adsorption performance utilising solely the structural degradation driven by thermochemical severity, entirely avoiding the use of toxic chemicals. Furthermore, studies focusing strictly on the energetic potential of agricultural waste often neglect the complexity of the generated liquid phase.

In this study, the implementation of an adsorbent resin column for the pretreatment and conditioning of the bio-oil directly addresses the challenge of pyrolytic liquid stabilisation. By removing non-phenolic impurities and heavy pyrolytic oligomers, the liquid phase was successfully refined, revealing a rich profile of valuable methoxyphenols and aromatic aldehydes. Crucially, comparing the thermochemical pathways reveals that hydrothermal carbonisation operates via subcritical water-mediated hydrolysis, yielding a highly selective oxygenated profile rich in monomeric phenolics and aldehydes. In contrast, dry pyrolysis relies on thermal cracking and deep deoxygenation at elevated temperatures, successfully eliminating oxygen to generate a diversified distribution spanning methoxyphenols and pure hydrocarbons. Recovering these target phenolics provides a sustainable,

Table 4
Comparison of biomass conversion strategies, product applications, and zero-waste alignment for various lignocellulosic residues.

Biomass Source	Conversion Strategy/ Treatment	Target Products & Applications	Zero-Waste Alignment & Process Limitations	Reference
Pistachio Shell (This Study)	HTC (250 °C-300 °C) & Pyrolysis (400 °C-500 °C) + Resin Pre-treatment	Multi-product: Biochar/hydrochar for dual use (Solid fuel, HHV: 31.81 MJ/kg & Dye Adsorbent, >96% removal) + Resin-conditioned Bio-oil (phenolic-rich).	High. No secondary toxic waste generated. Both solid and liquid phases are valorised without chemical activation.	Current Study
Pistachio & Almond Hulls	Single or Sequential Extraction (Microwave/Ultrasound)	Multi-product: Pectin, Phenolics, Exopolysaccharides (EPS), Single-cell protein (SCP).	Moderate to High. Focuses mainly on extraction and microbial conversion; solid residues require further downstream processing.	[26]
Pistachio Shells	Chemical Activation (KOH, $ZnCl_2$, H_3PO_4) & Pyrolysis	Single-product: Highly porous Activated Carbon for heavy metal and dye adsorption.	Low to Moderate. Generates secondary hazardous waste from chemical activating agents. The liquid phase is often neglected.	[27]
Peanut (Groundnut) Shells	Slow Pyrolysis (400-500 °C)	Single-product: Biochar for energy (Solid biofuel) and soil amendment.	Moderate. Focused only on the energetic and agricultural value of the solid fraction. Syngas and bio-oil were not structurally valorised.	[28]
Food Waste & Date Palm	Pyrolysis (350-650 °C) & Optimisation Modelling	Multi-product: Bio-oil and Biochar energy yield assessment.	High. Emphasises energy recovery (HHV modelling) but lacks specific environmental (adsorptive) application of the resulting biochar.	[29]
Hazelnut & Walnut Shells	Hydrothermal Carbonisation (HTC) & Biocomposite formulation	Single-product: Lignocellulosic fillers for polymer composites and bioplastics.	Moderate. Utilises the physical properties of the shell, but thermal degradation liquids are often treated as waste effluents.	[30]
Food Waste	Slow Pyrolysis (350 °C – 550 °C)	Single-product: Biochar for heavy metal remediation	Moderate. Solid biochar valorised; liquid/gas fractions unexploited (no multi-product refinery).	[31]
Pistachio Shells	Chemical Activation (KOH) & Pyrolysis	Single-product: Highly porous Activated Carbon for $CO_2 $ capture/gas adsorption.	Low to Moderate. Generates secondary hazardous waste from chemical activating agents; liquid phase is neglected.	[32]

bio-based alternative to fossil-derived aromatic precursors for advanced resin and adhesive synthesis. While this process successfully demonstrates the viability of zero-waste valorisation at a laboratory scale, further fundamental investigations are necessary to optimise resource efficiency. For instance, the aqueous phase of bio-oil (APBO) generated during HTC can be recirculated as the reaction medium for subsequent batches to minimise liquid waste. Additionally, high-temperature pyrolysis inevitably produces non-condensable gases (CO, CO_2, H_2, and CH_4) that hold significant calorific potential to supply partial endothermic heat for the pyrolysis reactor. Future studies should also focus on utilising advanced chromatographic separation on the conditioned bio-oil to precisely isolate specific commercial phenolic compounds. Ultimately, to scientifically validate the zero-waste claims of this model at a commercial scale, a comprehensive Life-Cycle Assessment (LCA) and Techno-Economic Analysis (TEA) are required to quantify the environmental footprint and economic competitiveness of the entire process from cradle to grave.

5. Conclusions

This study successfully demonstrates the holistic valorisation of pistachio hard shells, a highly abundant and underutilised agro-industrial residue, through a novel thermochemical biorefinery approach. By hydrothermal carbonisation (HTC) and high-severity dry pyrolysis with a first-of-its-kind adsorptive bio-oil conditioning step, the traditional linear waste disposal model is effectively replaced by a circular bioeconomy paradigm.

A significant contribution of this work lies in the unprecedented implementation of a specific macroporous adsorbent resin column (SEPLITE® LXA88) for the stabilisation and refinement of the complex liquid phase. To our knowledge, this is the first study to report the use of this specialised resin configuration for the treatment of thermochemical liquids derived from pistachio shells. This column proved to be an exceptional fractionation mechanism, successfully isolating target aromatic species from polar impurities and heavy oligomeric tars that typically mask analytical resolution. This refinement facilitated a high-resolution chemical profiling, revealing a remarkably rich distribution of high-value phenolic compounds, predominantly syringols (2,6-dimethoxyphenol) and methoxyphenols. These biogenic phenolics represent a critical renewable platform for the synthesis of advanced resins, adhesives, and antioxidants, offering a sustainable alternative to fossil-based aromatics.

The success of this proposed strategy is quantitatively validated across both solid and liquid phases, marking it as a uniquely comprehensive zero-waste model. In the solid phase, the peak thermochemical severity (dry pyrolysis at 500 °C) triggered deep deoxygenation and aromatisation, upgrading the raw biomass into a highly stable solid product with an exceptional Higher Heating Value (HHV) of 31.81 MJ/kg, proving its energetic equivalence to high-rank fossil fuels. Simultaneously, this biochar/hydrochar exhibited superior environmental performance, removing >96% of cationic Methylene Blue without the use of toxic chemical activating agents, thus surpassing the performance of many conventionally activated materials while avoiding hazardous effluents.

In conclusion, this study demonstrates that selecting the appropriate thermochemical pathway is critical depending on the target application: high-severity dry pyrolysis (500 °C) yields an optimal energy-dense biochar (HHV: 31.81 MJ/kg) with superior adsorptive properties, whereas hydrothermal carbonisation (250–300 °C) and resin conditioning effectively unlock valuable phenolic platform chemicals from the aqueous phase, establishing a comprehensive roadmap for the sustainable valorisation of pistachio shell residues.

Despite the promising dual-purpose valorisation achieved in this study, certain limitations should be noted, including the batch-scale operational constraints and the need to evaluate long-term column regeneration stability for macroporous resin conditioning. Future research directions should focus on scaling up these parallel thermochemical pathways into continuous-flow pilot systems, conducting comprehensive life cycle assessments (LCA), and optimizing techno-economic parameters for industrial-scale commercialisation.

Funding

This research received no external funding.

Declaration of competing interest

The authors declare that they have no known competing financial interests or personal relationships that could have appeared to influence the work reported in this paper.

Acknowledgments

The authors wish to express their deepest gratitude to Prof. Dr. Selhan Karagöz, Prof. Dr. Fahrettin Göğüş and Dr. Kubilay Tekin for their invaluable scientific guidance, insightful discussions, and technical support throughout this research. This study was carried out as part of a Master's thesis submitted to the Graduate School of Science and Engineering, Hacettepe University.

Appendix A

Table A1
GC-MS identification and relative distribution (Area %) of the chemical compounds in the refined liquid product derived from hydrothermal carbonisation of pistachio shells at 250 °C.

Phenols	**Area (%)**
Phenol, 2,6-dimethoxy-	65.11
Total	65.11
Aldehydes	**Area (%)**
Benzaldehyde, 4-hydroxy-3,5-dimethoxy-	34.89
Total	34.89

Table A2
GC-MS identification and relative distribution (Area %) of the chemical compounds in the refined liquid product derived from hydrothermal carbonisation of pistachio shells at 300 °C.

Phenols	**Area (%)**
Phenol, 2,6-dimethoxy-	52.87
Hydroquinone mono-TMS	11.36
Total	64.23
Acids	**Area (%)**
Benzenepropanoic acid, .alpha.-(1-hydroxyethyl)-.beta.-phenyl-	13.81
Total	13.81
Others	**Area (%)**
Benzenamine, 2-methoxy-4-nitro-	14.81
Carbazole	7.16
Total	21.97

Table A3
GC-MS identification and relative distribution (Area %) of the chemical compounds in the refined bio-oil derived from dry pyrolysis of pistachio shells at 400 °C.

Ketones	**Area (%)**
2-Propanone, 1-(acetyloxy)-	1.13
2-Cyclopenten-1-one, 2-methyl-	0.55
Ethanone, 1-(2-furanyl)-	0.41
2-Cyclopenten-1-one, 2-hydroxy-	2.11
1,2-Cyclopentanedione, 3-methyl-	3.01
Maltol	0.71
2-Cyclopenten-1-one, 3-ethyl-2-hydroxy-	0.83
2-Pentanone, 5,5-diethoxy-	0.57
Ethanone, 1-[4-(methylthio)phenyl]	0.42
4(5H)-Benzofuranone, 6,7-dihydro-3,6-dimethyl-, (R)-	2.88
Ethanone, 1-(4-hydroxy-3,5-dimethoxyphenyl)-	1.52
Total	14.14
Phenols	**Area (%)**
Phenol, 2,6-dimethoxy-	13.38
Hydroquinone mono-TMS	6.26
Phenol	0.66
Phenol, 2-methyl-	0.32
Phenol, 2-methoxy-	4.83
Phenol, 2-methoxy-4-methyl-	4.32
1,2-Benzenediol	3.99
1,2-Benzenediol, 3-methoxy-	1.64
Phenol, 4-ethyl-2-methoxy-	3.47

(*continued on next page*)

Table A3 (*continued*)

Eugenol	0.7
Phenol, 3,4-dimethoxy-	1
Phenol, 2-methoxy-4-propyl-	0.85
Phenol, 2-methoxy-4-(1-propenyl)-	0.4
Phenol, 2,6-dimethoxy-4-(2-propenyl)-	4.87
Total	46.69
Acids	**Area (%)**
3,5-Dimethoxy-4-hydroxyphenylacetic acid	2.35
Benzeneacetic acid, 4-hydroxy-3-methoxy-	0.96
Total	3.31
Alcohols	**Area (%)**
3-Furanmethanol	2.64
Total	2.64
Aldehydes	**Area (%)**
2-Furancarboxaldehyde, 5-methyl-	1.38
Ethyl Vanillin	0.48
Benzaldehyde, 4-hydroxy-3,5-dimethoxy-	0.95
3,5-Dimethoxy-4-hydroxycinnamaldehyde	0.43
Total	3.24
Esters	**Area (%)**
Butyrolactone	0.79
Total	0.79
Others	**Area (%)**
2H-Pyran, 3,4-dihydro-	0.33
2,4-Imidazolidinedione, 3-methyl-	0.83
Furan, 2-butyltetrahydro-	0.43
Furan, 2,5-diethoxytetrahydro-	3.47
2-Furaldehyde diethyl acetal	0.06
2-Butanamine	2.19
4-Methoxy-2-methyl-1-(methylthio)benzene	10.53
d-Allose	1.18
Benzeneethanamine, N-[(pentafluorophenyl)methyl]-	0.47
2,3-Dimethoxy-5-aminocinnamonitrile	0.35
Talbutal	0.32
Total	20.16

Table A4
GC-MS identification and relative distribution (Area %) of the chemical compounds in the refined bio-oil derived from dry pyrolysis of pistachio shells at 500 °C.

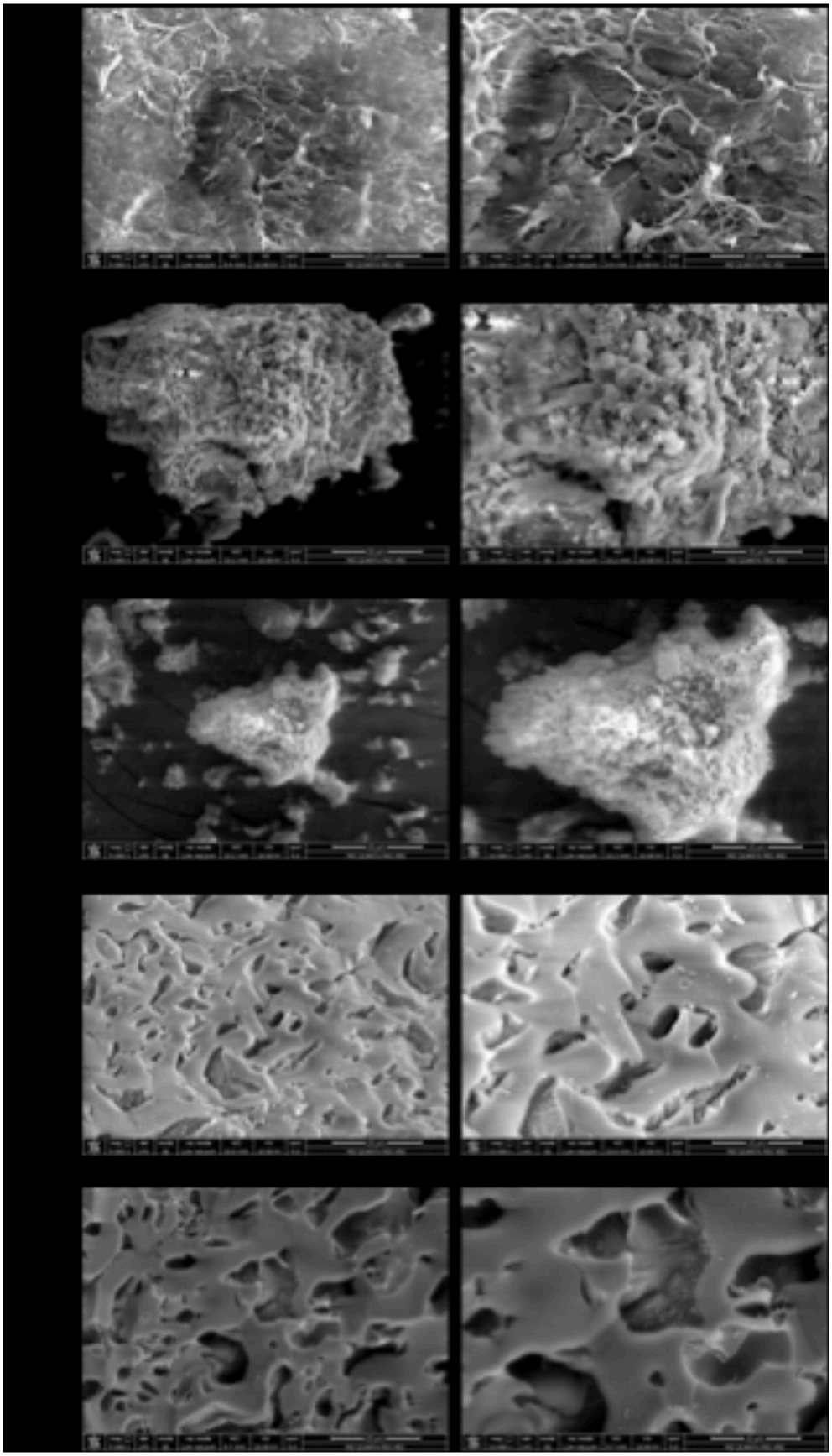
Ketones	**Area (%)**
2-Propanone, 1-(acetyloxy)-	1.04
2-Cyclopenten-1-one, 2-methyl-	0.68
Ethanone, 1-(2-furanyl)-	0.58
2-Cyclopenten-1-one, 2-hydroxy-	1.98
2-Butanone, 3,3-dimethyl-	0.49
2-Butanone, 1-(acetyloxy)-	0.26
2-Cyclopenten-1-one, 2-hydroxy-3-methyl-	2.53
2-Cyclopenten-1-one, 2,3-dimethyl-	0.27
Maltol	0.46
2-Cyclopenten-1-one, 3-ethyl-2-hydroxy-	0.61
2-Pentanone, 5,5-diethoxy-	0.54
2-Hydroxy-3-propyl-2-cyclopenten-1-one	0.24
2,5-Dihydroxypropiophenone	0.42
Ethanone, 1-(4-hydroxy-3-methoxyphenyl)-	0.47
4(5H)-Benzofuranone, 6,7-dihydro-3,6-dimethyl-, (R)-	3.29
Ethanone, 1-(4-hydroxy-3,5-dimethoxyphenyl)-	1.27
2-Pentanone, 1-(2,4,6-trihydroxyphenyl)	2.08
Total	17.21
Alkanaes-Alkenes-Alkines	**Area (%)**
3H-Benz[e]indene, 2-methyl-	0.52
Diphenylmethane	0.62
Total	1.14
Phenols	**Area (%)**
Phenol	1.59
Phenol, 2-methyl-	1.78
Phenol, 3-methyl-	2.27
Phenol, 2-methoxy-	4.11
Phenol, 2,4-dimethyl-	0.69
2-Methoxy-6-methylphenol	0.97

(*continued on next page*)

Table A4 (*continued*)

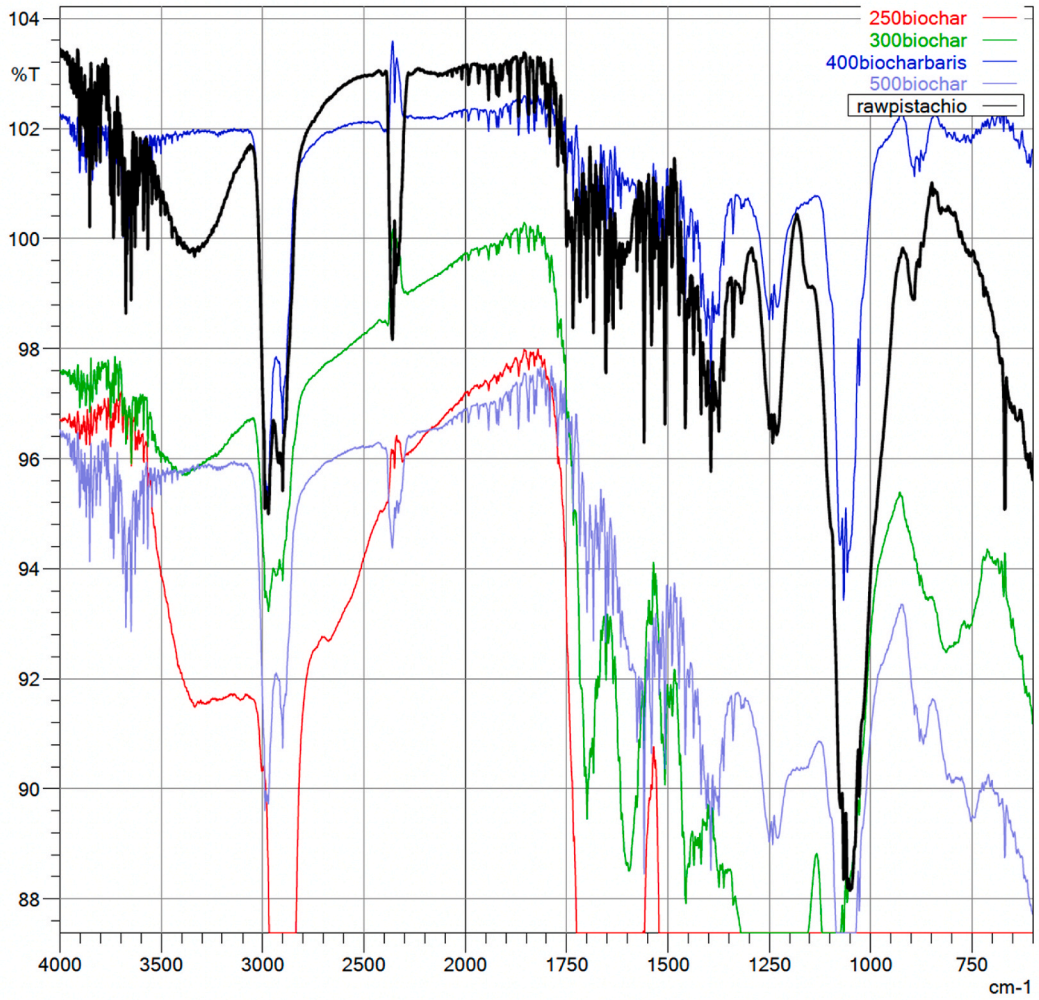
Phenol, 2-methoxy-4-methyl-	2.74
1,2-Benzenediol	3.18
Phenol, 2-ethyl-6-methyl-	0.29
1,2-Benzenediol, 3-methoxy-	1.88
1,2-Benzenediol, 3-methyl-	1.7
Phenol, 4-ethyl-2-methoxy-	2.74
Hydroquinone	0.26
1,2-Benzenediol, 4-methyl-	1.35
2-Methoxy-4-vinylphenol	0.31
Phenol, 2,6-dimethoxy-	9.15
3-Allyl-6-methoxyphenol	0.5
Phenol, 3,4-dimethoxy-	1.64
Phenol, 2-methoxy-4-propyl-	0.93
Phenol, 2-methoxy-4-(1-propenyl)-	0.3
Hydroquinone mono-TMS	4.92
Phenol, 2,6-dimethoxy-4-(2-propenyl)-	5.21
Total	48.51
Acids	**Area (%)**
3-Hydroxy-4-methoxybenzoic acid	7.95
Benzeneacetic acid, 4-hydroxy-3-methoxy-	1.48
Total	9.43
Alcohols	**Area (%)**
2-Furanmethanol	2.94
Ethanol, 2,2-diethoxy-	1.44
Total	4.38
Aldehydes	**Area (%)**
2-Furancarboxaldehyde, 5-methyl-	1.51
Benzaldehyde, 4-hydroxy-3,5-dimethoxy-	0.89
4-Hydroxy-2-methoxycinnamaldehyde	0.21
3,5-Dimethoxy-4-hydroxycinnamaldehyde	0.64
Vanillin	0.4
Total	3.65
Esters	**Area (%)**
Butyrolactone	0.62
2(5H)-Furanone	0.53
Octanoic acid, O-hydroxyphenyl ester	0.94
Total	2.09
Others	**Area (%)**
Oxazolidine, 2,2-diethyl-3-methyl-	0.69
1-.beta.-d-Ribofuranosyl-1,2,4-triazole-3-carboxamide-5'-phosphate	0.34
Acrolein,dimethyl acetal	0.28
Furan, 2,5-diethoxytetrahydro-	2.1
2,3-Anhydro-d-mannosan	0.33
Benzene, 2-fluoro-1,3,5-trimethyl-	0.47
2-Dimethylamino-6,7-dihydroimidazo[1,2-a][1,3,5]triazin-4(8H)-one	0.48
2,3-Dimethoxy-5-aminocinnamonitrile	0.29
Total	4.98

Appendix B



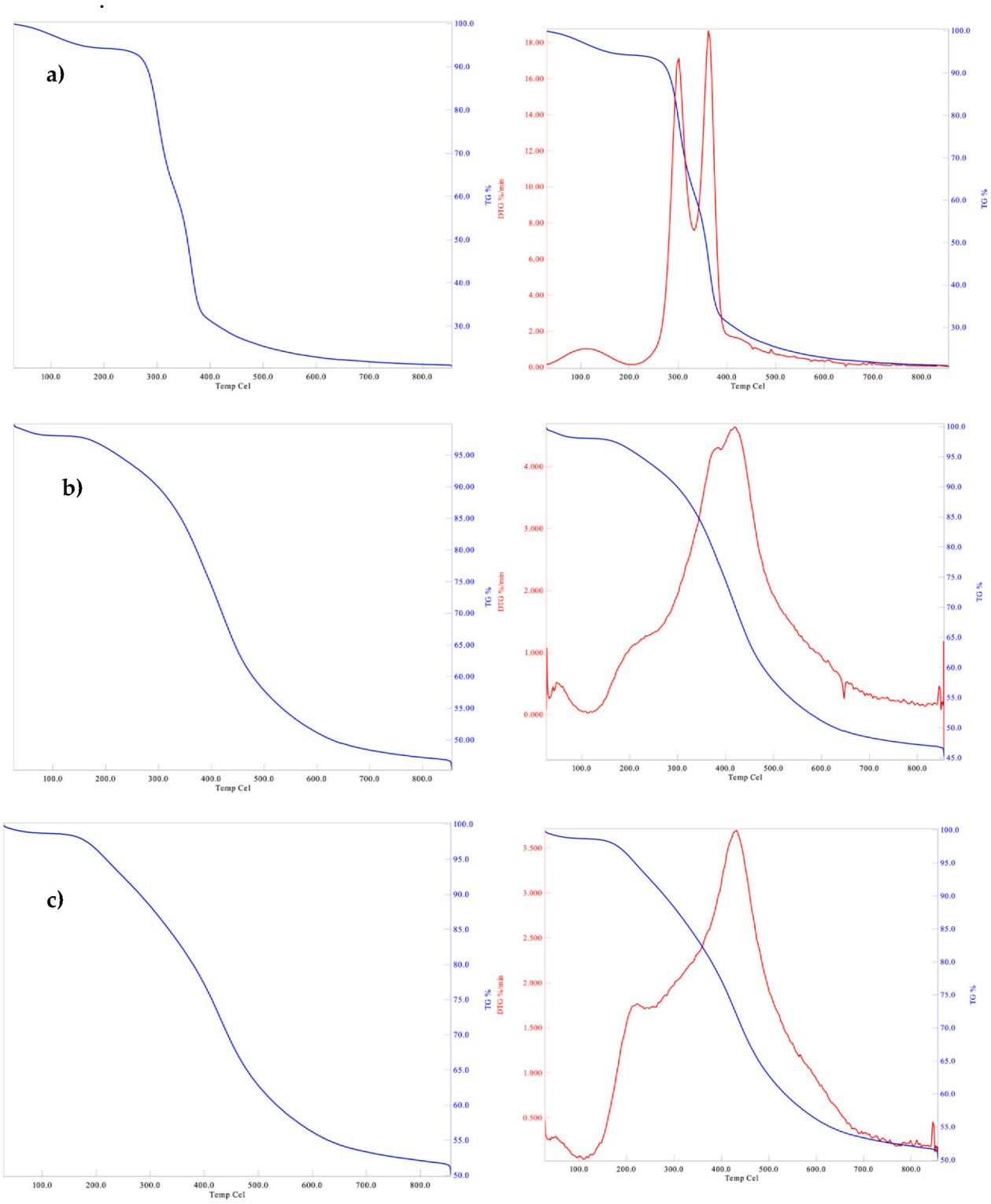
SEM Images of Solid Products. a) raw pistachio shells, b) 250 °C biochar c) 300 °C biochar, d) 400 °C biochar, e) 500 °C biochar.

Appendix C

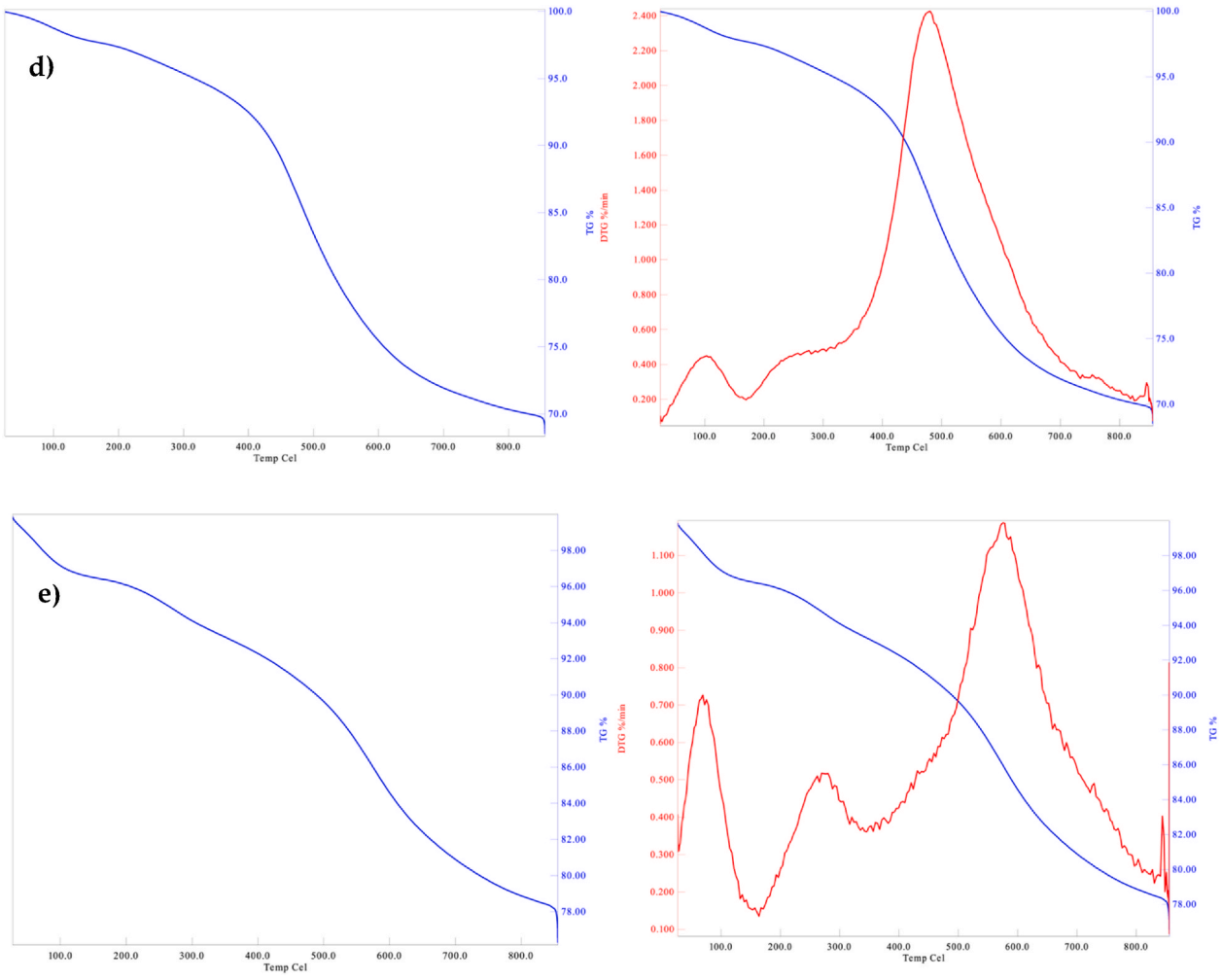


FTIR spectra of raw pistachio shells and biochars.

Appendix D



TG and DTG curves of materials a) raw pistachio shell b) 250 °C biochar c) 300 °C biochar d) 400 °C biochar e) 500 °C biochar.



Data availability

Data will be made available on request.

References

[1] Q. He, Q. Wang, J. Luan, A review on biomass pyrolysis and pyrolysis mechanisms, Biofuels 17 (3) (2026) 566–586.

[2] L. Dai, Y. Wang, Y. Liu, C. He, R. Ruan, Z. Yu, Q. Wu, A review on selective production of value-added chemi-cals via catalytic pyrolysis of lignocellulosic biomass, Sci. Total Environ. 749 (2020) 142386.

[3] N.M.P. Maklavani, M. Maskani, Systematic review of pistachio shell waste: environmental applications, sus-tainable approaches, and nanotechnology insights, Cleaner Waste Systems 10 (2025) 100219.

[4] S. Taheri, S.S. Hosseini, Waste not, want not: comprehensive valorization of fruit and vegetable waste from sin-gle-product recovery to zero-waste strategies, Cleaner Waste Systems 11 (2025) 100300.

[5] J. Toghiani, N. Fallah, B. Nasernejad, A. Mahboubi, M.J. Taherzadeh, N. Afsham, Sustainable pistachio dehull-ing waste management and its valorization approaches: a review, Curr. Pollut. Rep. 9 (1) (2023) 60–72.

[6] L. Fereidooni, A.R.C. Morais, M.B. Shiflett, Environmental applications of pistachio waste: a review, J. Environ. Manag. 380 (2025) 124927.

[7] K. Açıkalın, F. Karaca, E. Bolat, Pyrolysis of pistachio shell: effects of pyrolysis conditions and analysis of prod-ucts, Fuel 95 (2012) 169–177.

[8] S. Saghir, C. Pu, E. Fu, Y. Wang, Z. Xiao, Synthesis of high surface area porous biochar obtained from pistachio shells for the efficient adsorption of organic dyes from polluted water, Surf. Interfaces 34 (2022) 102357.

[9] S. Gupta, G.K. Gupta, M.K. Mondal, Thermal degradation characteristics, kinetics, thermodynamic, and reaction mechanism analysis of pistachio shell pyrolysis for its bioenergy potential, Biomass Convers. Biorefinery 12 (11) (2022) 4847–4861.

. (*continued*).

[10] S.A. Hassan, M. Abbas, S. Zia, A.A. Maan, M.K.I. Khan, A. Hassoun, R.M. Aadil, An appealing review of industrial and nutraceutical applications of pistachio waste, Crit. Rev. Food Sci. Nutr. 64 (10) (2024) 3103–3121.

[11] Z. Romero-Ceron, et al., Modified pistachio shell waste: structure, chemical interaction, and viscoelastic performance in biopolymer composites-based starch, Polym. Compos. 46 (9) (2025) 8025–8036.

[12] B. Ercan, K. Alper, S. Ucar, S. Karagoz, Comparative studies of hydrochars and biochars produced from ligno-cellulosic biomass via hydrothermal carbonization, torrefaction and pyrolysis, J. Energy Inst. 109 (2023) 101298.

[13] J. Petrović, M. Ercegović, M. Simić, M. Koprivica, J. Dimitrijević, A. Jovanović, J. Janković Pantić, Hydrothermal carbonization of waste biomass: a review of hydrochar preparation and environmental application, Processes 12 (1) (2024) 207.

[14] G. Ischia, H. Sudibyo, A. Miotello, J.W. Tester, L. Fiori, J.L. Goldfarb, Identifying the transition from hydro-thermal carbonization to liquefaction of biomass in a batch system, ACS Sustain. Chem. Eng. 12 (11) (2024) 4539–4550.

[15] I.G. Hakeem, P. Halder, M.H. Marzbali, S. Patel, S. Kundu, J. Paz-Ferreiro, K. Shah, Research progress on levoglucosan production via pyrolysis of lignocellulosic biomass and its effective recovery from bio-oil, Journal of Environ-mental Chemical Engineering 9 (4) (2021) 105614.

[16] Y. Wang, Y. Han, W. Hu, D. Fu, G. Wang, Analytical strategies for chemical characterization of bio-oil, Journal of separation science 43 (1) (2020) 360–371.

[17] T. Preechakun, S. Pongchaiphol, M. Raita, V. Champreda, N. Laosiripojana, Detoxification of hemicellu-lose-enriched hydrolysate from sugarcane bagasse by activated carbon and macroporous adsorption resin, Biomass Convers. Biorefinery 14 (2022) 14559–14574.

[18] Y. Li, et al., Adsorption study of lignin removal from recycled alkali black liquor by adsorption resins for improved cellulase hydrolysis of corn straw, Molecules 25 (19) (2020) 4475.

[19] J. Petrović, J. Janković, M. Ercegović, M. Simić, D. Radulović, Hydrothermal carbonization of waste biomass: a review of hydrochar preparation and environmental application, Processes 12 (2) (2024) 207.

[20] S. Masoumi, V.B. Borugadda, S. Nanda, A.K. Dalai, Hydrochar: a review on its production technologies and applications, Catalysts 11 (8) (2021) 939.

[21] S.K. Pereira, S. Kini, B. Prabhu, G.P. Jeppu, A simplified modeling procedure for adsorption at varying pH con-ditions using the modified Langmuir–Freundlich isotherm, Appl. Water Sci. 13 (1) (2023) 29.
[22] X. Zou, M. Zhai, D. Yang, G. Liu, T. Wang, L. Guo, Y. Zhang, New insights into the mechanism of biomass char steam gasification process by oxygen-containing functional group as aromatic carbon boundaries: experimental and DFT study, Chem. Eng. J. 465 (2023) 142947.
[23] Z. Li, Y. Jiang, Y. Li, H. Zhang, H. Li, S. Yang, Advances in Diels–Alder/aromatization of biomass furan deriva-tives towards renewable aromatic hydrocarbons, Catal. Sci. Technol. 12 (6) (2022) 1902–1921.
[24] S. Mandal, S. Adhikari, M. Murmu, B.H. Kim, D.H. Kim, Graphene and carbon quantum dots: competing carbons in harmonized photoelectrochemical platforms, Small 21 (40) (2025) e05846.
[25] K. Zhu, K. Li, Y. Zeng, Y. Wang, Y. Chen, Y. Zhang, K. Yan, Fundamentals of biomass-derived porous carbon, in: Fabrication and Applications of biomass-derived Porous Carbon, CRC Press, 2024, pp. 1–46.
[26] Z. Najari, F. Khodaiyan, M.S. Yarmand, S.S. Hosseini, Almond hulls waste valorization towards sustainable agricultural development: production of pectin, phenolics, pullulan, and single cell protein, Waste Management 141 (2022) 208–219.
[27] C.A. Igwegbe, J.O. Ighalo, S. Ghosh, S. Ahmadi, V.I. Ugonabo, Pistachio (Pistacia vera) waste as adsorbent for wastewater treatment: a review, Biomass Convers. Biorefinery 13 (10) (2023) 8793–8811.
[28] T.I.K. Mathabatha, A.N. Matheri, M. Belaid, Peanut shell-derived biochar as a low-cost adsorbent to extract cadmium, chromium, lead, copper, and zinc (heavy metals) from wastewater: circular economy approach, Circ. Econ. Sustain. 3 (2) (2023) 1045–1064.
[29] M.I. Awad, Y. Makkawi, N.M. Hassan, Yield and energy modeling for biochar and bio-oil using pyrolysis tem-perature and biomass constituents, ACS omega 9 (16) (2024) 18654–18667.
[30] S. Ollani, C. Peano, F. Sottile, Recent innovations on the reuse of almond and hazelnut by-products: a review, Sustainability 16 (6) (2024) 2577.
[31] A. Moureen, M. Waqas, N. Khan, F. Jabeen, C. Magazzino, N. Jamila, D. Beyazli, Untapped potential of food waste derived biochar for the removal of heavy metals from wastewater, Chemosphere 356 (2024) 141932.
[32] P.R. Chauhan, S.K. Tyagi, Experimental study on CO2 capture by KOH-activated pistachio shell char and its composites using chemisorption approach, Environmental Progress & Sustainable Energy 44 (4) (2025) e14638.
[33] W. Somyanonthanakun, A. Greszta, A.J. Roberts, S. Thongmee, Sugarcane bagasse-derived activated carbon as a potential material for lead ions removal from aqueous solution and supercapacitor energy storage application, Sustainability 15 (6) (2023) 5566.
[34] J. Yu, Y. Bian, R. Wang, S. Zhou, Z. Wang, D. Wang, H. Li, Coconut shell carbon preparation for rhodamine B adsorption and mechanism study, Molecules 29 (17) (2024) 4262.
[35] Z. Bao, V.F. Lotfy, X. Zhou, S. Fu, A.H. Basta, Assessment of porous carbon from rice straw residues with potassium ferrate-assisted activation as cationic and anionic dye adsorbents, Ind. Crop. Prod. 212 (2024) 118298.